

**ASSESSMENT OF THE INFLUENCE OF TIP SPEED RATIO,
SOLIDITY AND REYNOLDS NUMBER ON THE AERODYNAMIC
PERFORMANCE OF SELECTED LOCALLY FABRICATED WIND
TURBINES IN TANZANIA**

John Peter Kachira

**MSc (Physics) Dissertation
University of Dar es Salaam
March, 2019**

**ASSESSMENT OF THE INFLUENCE OF TIP SPEED RATIO,
SOLIDITY AND REYNOLDS NUMBER ON THE AERODYNAMIC
PERFORMANCE OF SELECTED LOCALLY FABRICATED
WIND TURBINES IN TANZANIA**

By

John Peter Kachira

**A Dissertation Submitted in Partial Fulfillment of the Requirements for the
Degree of Master of Science in Physics of the University of Dar es Salaam**

**University of Dar es Salaam
March, 2019**

CERTIFICATION

The undersigned certifies that he has read and hereby recommends for acceptance by the University of Dar es Salaam a Dissertation titled *“Assessment of the Influence of Tip Speed Ratio, Solidity and Reynolds Number on the Aerodynamic Performance of Selected Locally Fabricated Wind Turbines in Tanzania”*, in partial fulfillment of the requirements for the degree of Master of Science in Physics of the University of Dar es Salaam.

.....

Prof. R. R. Kainkwa
(Supervisor)

Date

**DECLARATION
AND
COPYRIGHT**

I, **John Peter Kachira**, declare that this dissertation is my own original work and that it has not been presented and will not be presented to any one for a similar or any other degree award.

Signature

This dissertation is copyright material protected under the **Berne Convention**, the copyright Act 1999 and other international and national enactments, in that behalf, on intellectual property. It may not be reproduced by any means, in part or in full, except for short extracts in fair dealing, for private study or research, critical scholarly review or discourse with an acknowledgement, without written permission of the Directorate of Postgraduate Studies, on behalf of both the author and the University of Dar es Salaam.

ACKNOWLEDGEMENTS

I would like to express my sincere thanks to my supervisor **Prof. R. R. Kainkwa** for devoting his time in providing guidance during both my coursework and dissertation. I appreciate his constructive criticism, commitment and knowledge imposition on my entire study period.

Let my sincere thanks go to Mbeya University of Science and Technology (MUST) via the office of academic research and consultancy for granting me financial assistance and study leave. I thank everybody who got involved in making sure I got this sponsorship.

I would like to give thanks to all Physics Department academic and non-academic staff of University of Dar es Salaam for their constructive instructions for the whole study period.

Let my sincere thanks go to MSc. students, Mr. L. Masanja, Mr. R. Mfaume, Mr. L. Charles, Mr. J. Hamad, Mr. Hafidh and Ms. D. Japhet, whom we cooperated together both during course work and dissertation stages.

Finally, let my sincere thanks go to local wind turbines craftsmen, Mr. Mchau, Mr. Matiya and Mr. Kyando for providing me with horizontal axis wind turbines blades from their windmill enterprises for data acquisition toward completion of this work.

DEDICATION

To my wife

Lukrecia Lucas Nzohumpa

And

My Daughters,

Ishimwe Glory, Ndizeye Angel

And

Hakizimana

LIST OF ABBREVIATIONS

AGL	Above Ground Level
BEMT	Blade Element Momentum Theorem
CAMARTEC	Centre for Agricultural Mechanization and Rural Technology
CoNAS	College of Natural and Applied Sciences
HAWT	Horizontal Axis Wind Turbine
IPI	Institute of Production Innovation
NACA	National Advisory Committee for Aeronautics
NEC	National Engineering Company
RPM	Revolution Per Minute
TSR	Tip Speed Ratio
VAWT	Vertical Axis Wind Turbine
WECS	Wind Energy Conversion Systems

LIST OF SYMBOLS

α	Angle of Attack
ω	Velocity of a Wind Rotor
P_a	Available Wind Power
c	Chord Width
C_d	Drag Coefficient
D	Drag Force
P_e	Extractable Wind Power
η	Kinematics Air Viscosity
C_l	Lift Coefficient
L	Lift Force
S	Length of Disturbed Wind
$C_{p \max}$	Maximum Power Coefficient
C_p	Power Coefficient
R	Radius of the Rotor
Re	Reynolds Number
σ	Solidity
V_∞	Velocity at Infinite

ABSTRACT

The sites with good wind energy conditions in Tanzania have motivated some local craftsmen to manufacture wind turbines using local and imported materials. However, some studies have shown that these turbines have low performance. In this study, theoretical approach has been carried out to assess the influence of TSR, solidity and Re on the aerodynamic performance of nine selected locally fabricated wind turbines in Tanzania. Three manufacturing centers namely, Dar es Salaam, Singida and Makambako were selected and three different HAWT rotor blades from each center were put under testing. Their respective rotor radii and chord widths were measured and used to determine their TSR, solidity and Re .

The measured TSRs were 0.63, 0.70, 0.79, 0.90, 1.57, 2.09, 2.51, 3.14, and 4.19. Unlike 4.19, the rest values were below the recommended range between 4 and 10 for which WECS are recommended to generate large scale electricity. The respective measured solidities were, 0.90, 0.10, 0.13, 0.17, 0.18, 0.28, 0.88, 1.07 and 1.22. These solidities were found to be above the proposed range between 0.01 and 0.05 for which WECS are designed to generate large scale electricity. These high solidities lead into high torques reducing rotational speed of the WECS. The measured Re_s were 86,030, 99,265, 100,589, 102,574, 125,736, 138,972, 145,589, 145,589 and 152,207. These Re values are below the standard Re which is at least 1×10^6 implying that they exhibit turbulent flow with high level of drag coefficient that influences low performance of the WECS. The 3 - bladed wind turbine from Matiya in Singida was found to have good TSR of 4.19 though its solidity was found to be above the recommended standard values range. It needs an optimization of its chord and radius to improve its efficiency. Therefore, these wind turbines can only generate small scale electricity due to their poor aerodynamic performances.

TABLE OF CONTENTS

Certification	i
Declaration and Copyright	ii
Acknowledgements	iii
Dedication	iv
List of Abbreviations	v
List of Symbols	vi
Abstract	vii
Table of Contents	viii
List of Tables	x
List of Figures	xi
CHAPTER ONE: INTRODUCTION	1
1.1 General Introduction	1
1.2 Statement of the Problem	3
1.3 Research Objectives	3
1.4 Research Questions	4
1.5 Significance of the Research	4
CHAPTER TWO: LITERATURE REVIEW	5
2.1 Introduction	5
2.2 Categories of Wind Turbines	5
2.3 Wind Turbine Technology in Tanzania	7
2.4 Performance of Locally Fabricated HAWTs	8
2.5 Blade Airfoils Uniqueness	9
2.6 Forces That Govern Working Principle of a HAWT Blade	11
2.7 Blade Plan Regions and Chord Length Linearization	13
2.8 Blade Twist Angle and the Acting Load	19
2.9 Power Coefficient of a HAWT	25
2.10 Solidity of a Wind Turbine	27
2.11 Tip Speed Ratio of a Rotor	28

CHAPTER THREE: MATERIALS AND METHODS	31
3.1 Introduction.....	31
3.2 Materials	31
3.2.1 Study Site	31
3.2.2. Wind Turbine Blades	31
3.3 Methods for Determination of TSR, Solidity and Re Parameters.....	36
CHAPTER FOUR: RESULTS AND DISCUSSIONS.....	38
4.1 Introduction.....	38
4.2 Measured Parameters of Local HAWTs	38
4.2.1 Measured TSRs	38
4.2.2 Measured Solidities.....	39
4.2.3 Measured Re	39
4.2.4 Comparison of this Study Results with Other Studies in Tanzania	40
CHAPTER FIVE: CONCLUSIONS AND RECOMMENDATIONS	43
5.1 Introduction.....	43
5.2 Conclusions.....	43
5.3 Recommendations.....	43
REFERENCES.....	44
APPENDICES	48

LIST OF TABLES

Table 3.1:	Recommended Blade Design Parameters for Large Scale Electricity Generation	36
Table 4.1:	Measured TSRs, Solidities and Re_s of Local HAWTs.....	38
Table 4.2:	Comparison of Measured TSR, Solidity and Re with Other Studies in Tanzania	41

LIST OF FIGURES

Figure 2.1:	Standard Horizontal Axis Wind Turbine.....	5
Figure 2.2:	Standard Vertical Axis Wind Turbine.....	6
Figure 2.3:	Cambered Airfoil	9
Figure 2.4:	Different Forms of Airfoils	10
Figure 2.5:	Definition of Lift and Drag	11
Figure 2.6:	Generation of Lift in an Airfoil Wind Turbine Blade	12
Figure 2.7:	A Typical Blade Plan and Region Classification	14
Figure 2.8:	Efficiency Losses Due to Ideal Chord Width Simplification	14
Figure 2.9:	A Typical Modern HAWT Blade showing, (a) Linear Chord Length, (b) Twist Angle and (c) Multiple Aerofoil Profiles	15
Figure 2.10:	Chord Length of a Wind Turbine Blade	16
Figure 2.11:	Optimum Chord Distribution	17
Figure 2.12:	Uniform Taper Blade Design for Optimal Operation.....	18
Figure 2.14:	Blade Twist Angle and Velocities at the Rotor Plane	20
Figure 2.15:	Optimum Pitch Angle Distribution	21
Figure 2.16:	Loading Caused by the Earth’s Gravitational Field	22
Figure 2.17:	Loading Caused by Braking the Rotor	23
Figure 2.18:	Effect of Coning the Rotor	24
Figure 2.19:	Sketch of Turbulent Inflow Seen By Wind Turbine Rotor	25
Figure 2.20:	Torque Coefficient for TSR Sketched for Large Solidity, Small Solidity and Ideal Criterion	27
Figure 2.21:	Influence of the Number of Blades on Rotor Power Coefficient and Optimum Tip Speed Ratio	29
Figure 3.1:	6 - Bladed HAWT.	32
Figure 3.3:	20 - Bladed HAWT.	33
Figure 3.4:	3 - Bladed HAWT.	33
Figure 3.5:	4 - Bladed HAWT.	34
Figure 3.7:	16 - Bladed HAWT.	35
Figure 3.8:	18 - Bladed HAWT.	35
Figure 3.9:	14 - Bladed HAWT.	36

CHAPTER ONE

INTRODUCTION

1.1 General Introduction

Locally fabricated wind turbines industry in Tanzania is growing day by day as the number of craftsmen dealing with small stand - alone wind energy systems is increasing. The most popular craftsmen are in Makambako, Dar es Salaam, Singida, Songea and Manyara (Msuya, 2015). These craftsmen fabricate various types of wind turbines and windmills using locally available and few imported materials. Most of the locally fabricated wind turbines have low efficiency and as a result they have poor performance compared to the standard wind turbines (Talam, 2011 and Msuya, 2015). These authors argued that the low efficiency is caused by a number of factors including bad arrangement of the blades, poor geometry of blades; nature of material used and design parameters. The design parameters include among others the rotor diameter, chord distribution and twist of the blade. These design parameters add to aerodynamic drag and boundary layer separation if not properly designed. They further suggested that the local craftsmen need more technical skills that would help them to optimize their wind turbines.

To improve these wind turbines there is a need to pay more attention to the rotor blade which is the most important part of a wind turbine for capturing wind. Normally the blade must be airfoil shaped to efficiently convert the wind's kinetic energy to rotational energy. The blade performance is influenced by different design parameters including Tip Speed Ratio (TSR), number of rotor blades, optimum shape of the rotor blade, rotor blade thickness, solidity, Reynolds number (Re) as well as nature of the material (Cagle et al. 2007). According to Tony et al (2001), Reynolds number is a unit less number applied in fluid mechanics to indicate whether fluid flow past a body or in a duct is steady or turbulent. For the case of wind energy the Re indicates how steady or turbulent the air flow past a blade of a wind turbine is. Assessment of the local wind turbine parameters in comparison to the standard design levels would help to improve performance of the rotor blades of these local wind turbines. Knowledge of rotor blade materials used is also necessary to improve performance of the locally fabricated wind turbines. Thus, for optimal wind turbine

blade performance, materials for the design of wind turbines rotor blades should meet the following criteria as Hansen (2008) suggested: trouble free processing to reduce maintenance cost, low density to diminish gravitational forces, high strength to withstand strong loading of wind, high fatigue resistance to withstand cyclic loading, high stiffness to ensure stability of the optimal shape and orientation of the blade, high fracture toughness, the ability to withstand environmental impacts such as lightning strikes, humidity and temperature. Metals would be unwelcome because of their vulnerability to fatigue. Ceramics have low fracture toughness, which could result in early rotor blade failure. Traditional polymers are not rigid enough to be useful, and wood faces problems of swelling and elongation especially considering blade length when subjected to wetting due to water. The author concluded that this leaves fibre-reinforced composites, which have high strength and stiffness and low density, as a very attractive class of materials for the design of wind turbines.

The rotor blades of locally fabricated wind turbines are not optimized for improved power output efficiency (Msuya, 2015). Aerodynamic optimization of blade airfoil is essential in the design of a wind turbine in order to obtain optimal power coefficient at the design wind speed (Eke and Onyewudiala, 2010). The nature of performance of the rotor aerodynamics is based on the power output of the wind turbine at a particular wind speed. Finding the best possible design for the geometric shape of the rotor can be done by taking into reflection aerodynamic performance, strength and stiffness necessities and inexpensive production techniques (Habali and Saleh, 1995).

The efficiency of a wind turbine can be improved by modifying the number blades of a rotor, optimum shape of the rotor blade, blade thickness, solidity, Reynolds number and design TSR of the rotor (Cagle et al. 2007). For the case of the rotor blade shape, the wind turbine must be designed in such a way that, for use at high turbulent wind region it must have smaller diameter rotor and more robust than wind turbines for lower wind regions (Talam 2011). Therefore, this study focused on the tip speed ratio, solidity and Reynolds number parameters of the blades of selected Horizontal Axis Wind Turbines (HAWTs) fabricated in three centers namely Dar es Salaam,

Makambako and Singida. These parameters need to be studied since they are known to significantly affect the blade performance of the wind turbine.

1.2 Statement of the Problem

The sites with good wind energy conditions in Tanzania have motivated some local craftsmen to apply their indigenous knowledge to develop and manufacture wind turbines using locally available and imported materials. However, some studies have revealed that the locally fabricated wind turbines have low performance (Talam, 2011 and Msuya, 2015). The low performance is likely due to poor aerodynamic blade designs, poor materials used and bad blade arrangement where the shapes of the blades used are not airfoil. The way the turbine blades are fixed to the rotor also contributes to the loss in energy due to wake effect created by high torque. The blade parameters especially the tip speed ratio, solidity and Reynolds number are known to have great influence on low aerodynamic performance of blades, yet they have not been sufficiently studied for subsequent improvement of the local wind turbines. This study therefore, aims at assessing the influence of tip speed ratio, solidity and the Re on the aerodynamic performance of selected locally fabricated wind turbines that can give some light toward improvement of the aerodynamic performance of the locally fabricated wind turbines.

1.3 Research Objectives

The main objective of this study was to assess the influence of tip speed ratio, solidity and Reynolds number on the aerodynamic performance of selected locally fabricated wind turbines in Tanzania. The specific objectives of this study were:

- i. To investigate the influence of Tip Speed Ratio on the aerodynamic performance of selected locally fabricated horizontal axis wind turbines.
- ii. To evaluate the effect of solidity on the aerodynamic performance of selected locally fabricated horizontal axis wind turbines.
- iii. To assess the influence of Reynolds number on the aerodynamic performance of selected locally fabricated horizontal axis wind turbines.

1.4 Research Questions

The proposed study intended to provide answers to the following questions:

- i. How does Tip Speed Ratio influence aerodynamic performance of locally fabricated horizontal axis wind turbine?
- ii. How does solidity affect the aerodynamic performance of locally fabricated horizontal axis wind turbine?
- iii. How does Reynolds number influence the aerodynamic performance of locally fabricated horizontal axis wind turbine?

1.5 Significance of the Research

The results of this study may provide information to local wind turbines craftsmen on how Tip Speed Ratio, solidity and Reynolds number parameters influence the efficiency of locally fabricated HAWTs. The results may be used to suggest ways on how the craftsmen can improve the performance of their local wind turbines. The results may also pave way to increased use of these locally fabricated wind turbines. The performance of these locally fabricated wind turbines can be improved by choosing optimal chord width and shape of a blade that conform to the optimal TSR, solidity and Re parameters.

CHAPTER TWO

LITERATURE REVIEW

2.1 Introduction

This chapter presents an overview of the past literatures and theories concerning aerodynamic systems of wind turbines for electricity generation. The chapter reports categories of wind turbines, wind turbine technology in Tanzania, performance of locally fabricated wind turbine, forces that govern the working principle of a horizontal axis wind turbine, power coefficient of horizontal axis wind turbines, solidity of a wind turbine, Tip Speed Ratio of a rotor, blade airfoils uniqueness, blade plan shape regions and chord length linearization, blade twist angle and loads that act on a wind turbine blade.

2.2 Categories of Wind Turbines

There are two main categories of wind turbines namely, Horizontal Axis Wind Turbines (HAWTs) and Vertical Axis Wind Turbines (VAWTs). They are categorized as such depending on the orientation of the axis of rotation of a rotor (Gipe, 1993). Figure 2.1 shows a HAWT in which the axis of rotation is horizontal to the ground.

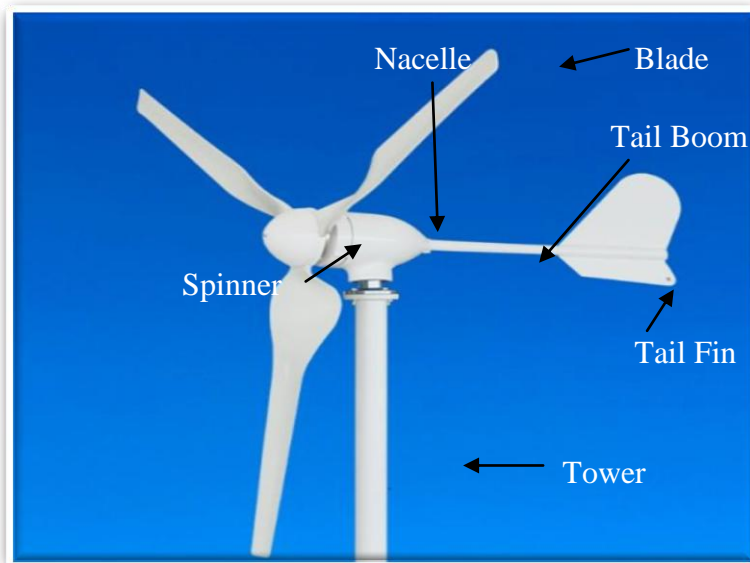


Figure 2.1: Standard Horizontal Axis Wind Turbine. Source: <https://www.google.com>.

Figure 2.2 depicts a VAWT in which the axis of rotation is vertical to the ground and perpendicular to the wind direction. The use of yaw mechanism is not necessary for this type of Wind Energy Conversion Systems (WECS) because it can receive wind from any direction (Hansen 2008). Both the generator and the gearbox of such systems can be built at the ground level, making the tower design easy and cheaper. Moreover, the maintenance of these turbines can be done at the ground level. However, VAWT do not take the advantage of stronger winds at higher elevation as the HAWT do.



Figure 2.2: Standard Vertical Axis Wind Turbine. Source: <https://www.google.com>.

Both types of wind turbines have diverse applications in generating power and utility operation from domestic usage to large scale wind farm (Spera, 1998). The author reported that these types of wind turbines can be classified as either small scale, medium scale or large scale. Small scale wind turbines usually have rotor diameter of less than 12 m and power rating less than 50 kW. Medium scale wind turbines should

have rotor diameter between 12 m and 45 m with power rating between 50 kW to 999 kW. Large scale wind turbines should have rotor diameter of at least 46 m and power rating of at least 1 MW.

2.3 Wind Turbine Technology in Tanzania

The technology of harvesting wind energy is not well established in Tanzania though there have been many attempts to develop wind turbine systems for harnessing wind energy (Msuya, 2015). There are a number of institutions that depict development of wind energy technology in Tanzania like ‘Ujuzi Leo Industry’ company in Arusha. This company manufactured WECS for water pumping but the report depicted that this machine lacked control at high speeds and its efficiency was also not known (Kihedu, 2007).

The Institute of Production Innovation (IPI) that was housed at the College of Engineering and Technology at the University of Dar es Salaam, and the National Engineering Company (NEC) together constructed a Savonius wind machine for pumping water (Talam, 2011 and Msuya, 2015). The Center for Agricultural Mechanization and Rural Technology (CAMARTEC) also has been dealing with wind energy technology by designing and manufacturing windmills although the technology couldn’t reach commercial stage due to financial shortage. The investigation report on installed windmills in thirteen regions of Tanzania mainland by Nzali and Mushi (2006) revealed that 44 % of the windmills were actively working while 56 % were not working and their efficiencies were not known as well.

Kainkwa and Mwanyika (2006) reported that there were local technicians at Makambako in the Southern part of Tanzania who were engaged in designing and manufacturing local wind turbines using bicycle wheels and dynamo. The local wind turbines fabricated could generate electricity limited to household lighting and other domestic appliances. The output from the dynamo was connected to a battery as power bank for the purpose of obtaining a constant power supply (Msuya, 2015).

There are famous local WECS engineering enterprises in Tanzania mainland namely; Mchau windmill enterprise in Dar es Salaam, Kyando windmill enterprise in Makambako and Matiya windmill enterprise in Singida (Talam 2011 and Msuya, 2015). The craftsmen in these enterprises manufacture their wind turbine blades using plastics, metal and fibre. Some of these materials are locally available and some for instance, permanent magnets are from abroad. The local craftsmen also amend scrap generators from washing machines, used cars, broken motors and motorcycles to construct generators for WECS (Msuya, 2015).

2.4 Performance of Locally Fabricated HAWTs

The performance of locally fabricated HAWTs was reported to be poor because the turbines have low design tip speed ratios and corresponding high design solidities compared to the standard values (Talam, 2011). The author assessed the power output characteristics of two HAWTs turbines, one with a rotor of 5 blades and the other with 16 blades. The power coefficients of these machines were found to be 0.14 and 0.21 at TSRs of 0.61 and 1.7 as well as solidities of 0.5 and 0.29 respectively while modern HAWTs are designed with power coefficient in the optimal range of 0.4 to 0.5 (Cetin et al, 2001 and Hansen, 2008). Furthermore, the solidities of modern HAWTs are recommended to be less than 0.07 (Cetin et al, 2001, and Talam, 2011). Talam (2011) in his report concluded that the values of solidity and TSR he had obtained for the 5 and 16-bladed selected wind turbines were not suitable for large scale electricity generation because they were out of the optimal design range. The author further recommended improving the aerodynamic efficiencies of the machines by enhancing the interaction between scientists, engineers and indigenous technicians.

Msuya (2015) investigated the simulation of two generators, one local generator and one standard generator with 8 and 6 pole pairs respectively. The experimental results revealed that the Tanzanian locally fabricated generator had low efficiency since it recorded 55 % efficiency while the standard one recorded 96 % efficient both at 350 RPM (Msuya, 2015). The author further reported that the generator with six pole pair was better than the 8 pole pair by 31 %.

2.5 Blade Airfoils Uniqueness

There are many wind turbine blade cross sections design forms. There are those which are cambered and that which is none cambered. Camber is defined as the asymmetry between two acting surfaces of an airfoil with the top surface of a wing commonly being more convex as depicted in Figure 2.3. Any aerofoil which is not cambered is known as a symmetric aerofoil (Jansen and Smulder, 1977). By observation from Figure 2.3, it can be shown that, both leading edge and the trailing edge are separated by a chord c . The leading edge is the fraction of the airfoil that first contacts the air; in other words it is the foremost edge of an airfoil section, while the trailing edge is the back edge of the blade, where airflow separated by the leading edge comes together over again. Chord is an imaginary line that combines the leading and trailing edges. Operation purpose for which a wind turbine is intended has a vital importance on selection of the shape and design of the blade for wind turbine (Jansen and Smulder, 1977). The authors further reported that for a wind turbine designed for low speeds, a thick airfoil is the most preferred, while a thin airfoil is best for high speeds.

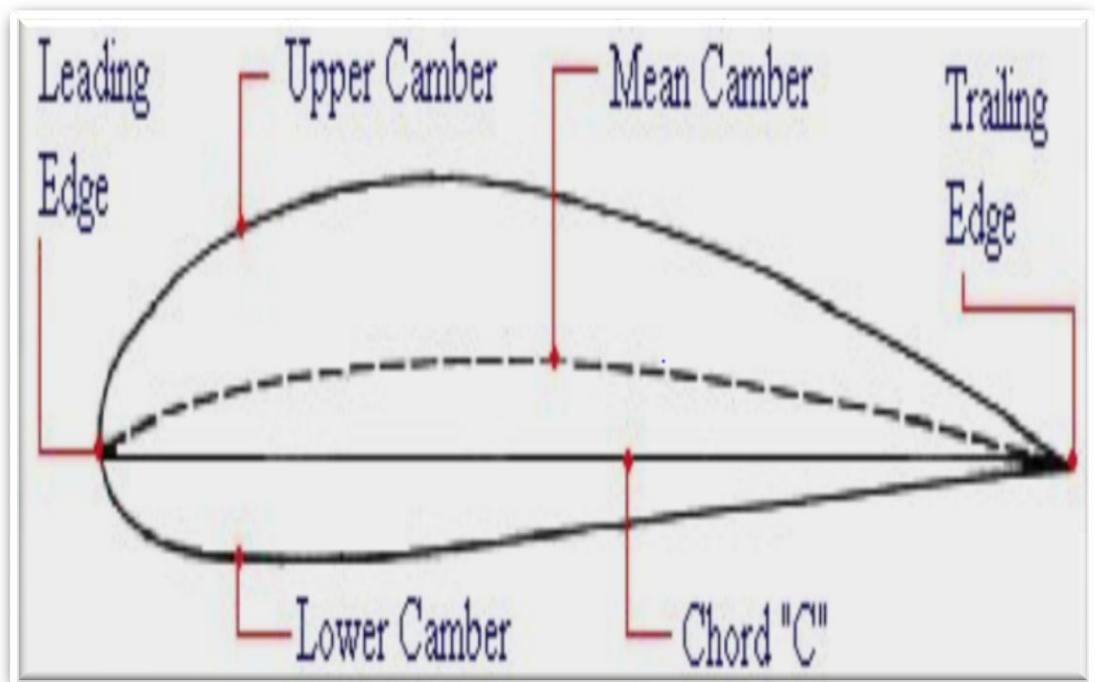


Figure 2.3: Cambered Airfoil (Jansen and Smulder, 1977).

Figure 2.4 shows wind turbine blades cross sections of different design forms. According to Hansen (2008), commonly used airfoil forms over the past decades for HAWTs include the NACA 44XX, NACA 23XXX, NACA 63XXX and NASA LS (1) series airfoils. The NACA 4 digit airfoils implies that the first digit expresses the camber in percent chord, the second digit gives the maximum camber point location in tenths of chord while the last two digits give the thickness in percent chord. The NACA 5 digit series airfoil means that the first digit designates the approximate camber in percent chord, the second digit indicates twice the position of camber tenths chord, the third either, 0 or 1 distinguishes the type of mean camber line and the last two digits give the thickness in percent chord.

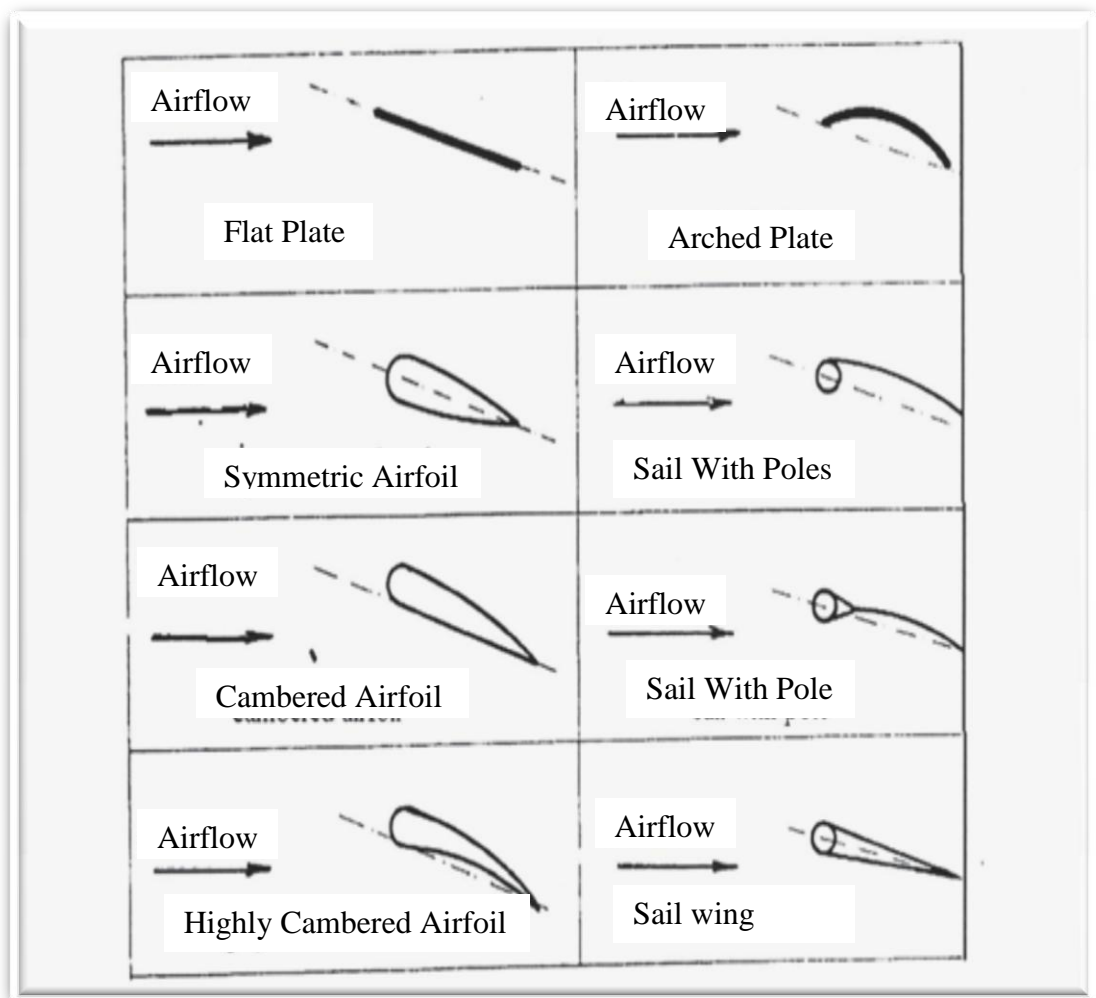


Figure 2.4: Different Forms of Airfoils (Jansen and Smulder, 1977).

2.6 Forces That Govern Working Principle of a HAWT Blade

Principally there are two forces essential for rotating the rotor of a HAWT. The reacting force \mathbf{F} from the flow strikes on the leading edge toward the trailing edge of the airfoil and is then decomposed into directions perpendicular and parallel to the velocity at infinity, V_∞ . The former component is known as the lift, L and the latter is called the drag, D .

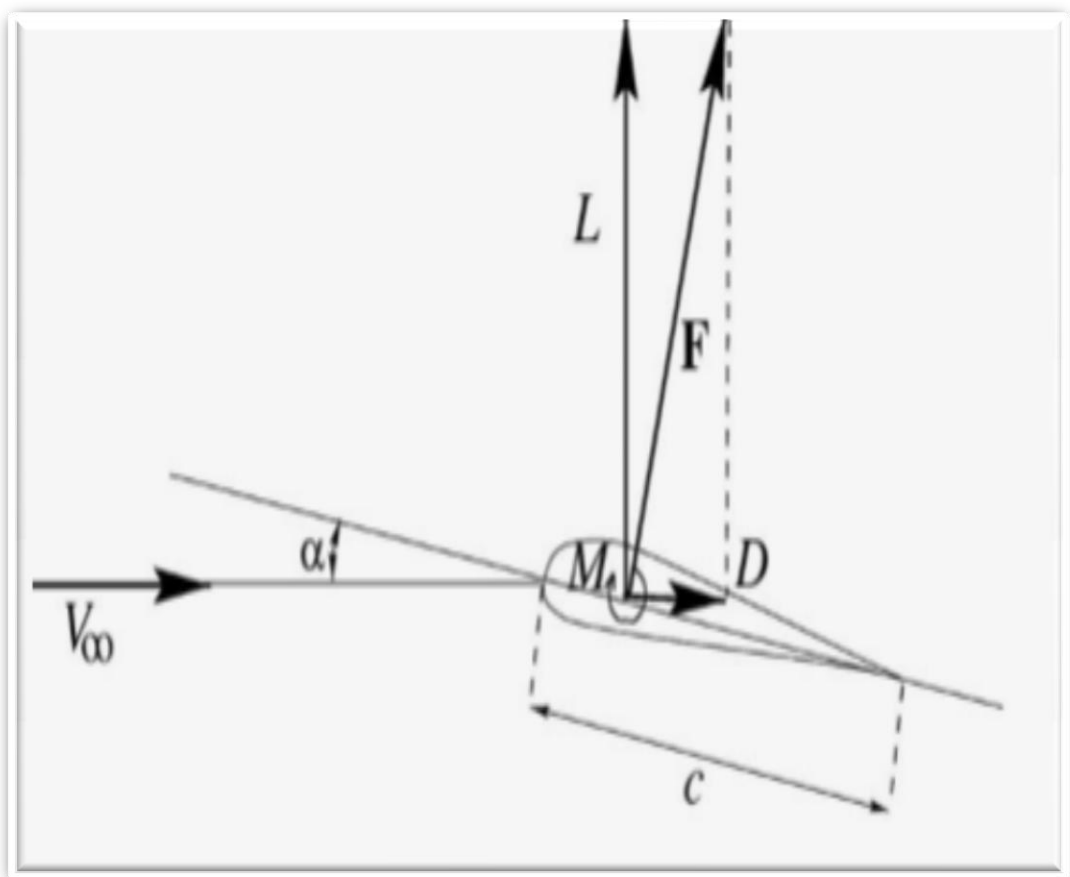


Figure 2.5: Definition of Lift and Drag (Hansen 2008).

According to Hansen (2008), the drag force acts in the direction of incoming wind thereby striking and pushing the rotor blade about its axis, while the lift force results from the Bernoulli's principle whereby pressure difference created by air flowing over a blade as shown in Figure 2.6 results in lift force. The lift and drag coefficients are measured as a function of the angle of attack (Spera, 1998). The author further reported that at the critical angle of attack at which the flow separates from the top of

the airfoil, the lift to drag coefficient ratio becomes maximum. The effect of the turning moment on the blade is expressed using the aerodynamic force and moment coefficients being plotted in the polar airfoil curves (Hau, 2006). These curves are influenced by airfoil geometry and the Reynolds number Re . At higher Re , all of the airfoils exhibit better performance, such as higher lift coefficient, lower drag coefficient and larger lift-to-drag ratio at a given angle of attack (Hau, 2006). Higher Re of at least 1×10^6 indicate very good aerodynamic performance of a wind turbine (Hansen, 2008).

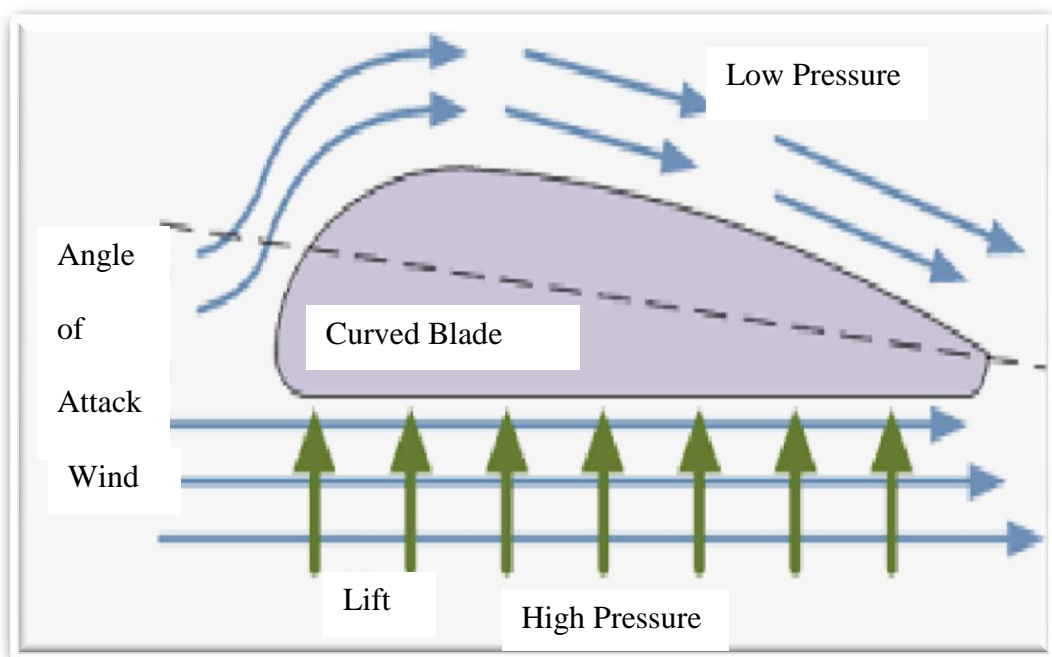


Figure 2.6: Generation of Lift in an Airfoil Wind Turbine Blade (Hansen 2008).

The nature of flow prototype around an airfoil can be determined by Re and this significantly affects the standards of the lift and drag coefficient. Drag coefficient general level increases with decreasing Re . The effect of lift coefficient is largely anxious with the angle of attack at which stall occurs. As Re increases so does stall angle and because the lift coefficient increases linearly with angle of attack below the stall, the maximum value of lift coefficient also increases (Hansen, 2008). According to Tony et al. (2001), for high Re , viscous forces are low and vice versa. The author depicted that Re is given by the relation:

$$Re = \frac{V \times c}{\eta} \dots\dots\dots (2.1)$$

where, η is kinematic air viscosity (m^2/s), V is the velocity of the fluid whereas c is the chord length of an airfoil.

The efficiency and control characteristics of fast turning wind rotors are determined to a greater extent by the aerodynamic properties of the airfoils used. Lift to Drag ratio, (L/D) is the most important parameter that characterizes critically the shape of the blade of a wind turbine and is expressed as (Hansen and Butterfield, 1993):

$$\frac{L}{D} = \frac{C_l}{C_d} \dots\dots\dots (2.2)$$

where, C_l and C_d are lift and drag coefficients respectively.

2.7 Blade Plan Regions and Chord Length Linearization

Modern blades can be divided into three main parts classified by aerodynamic and structural function (Hau, 2006). These are mid span, root, and tip as shown in Figure 2.7. The blade root is the switch between the circular mount and the first aerofoil profile. This part carries the highest load. It always experiences low wind velocity due to its small rotor radius. Low wind velocity at this part leads to reduced aerodynamic lift leading to large chord lengths. Therefore the blade profile becomes excessively large at the rotor hub. The problem of low lift is compounded by the need to use excessively thick aerofoil sections to advance structural reliability at this load severe region.

Therefore the root region of the blade typically consists of thick aerofoil profiles with low aerodynamic efficiency. The next region, mid span, is an aerodynamically significant part for which the lift to drag ratio is maximized thereby utilizing the thinnest possible aerofoil section that structural considerations allow. The last part, tip, is an aerodynamically critical part for which the lift to drag ratio is maximized, therefore, using slender airfoils and specially designed tip geometries to reduce noise and losses.

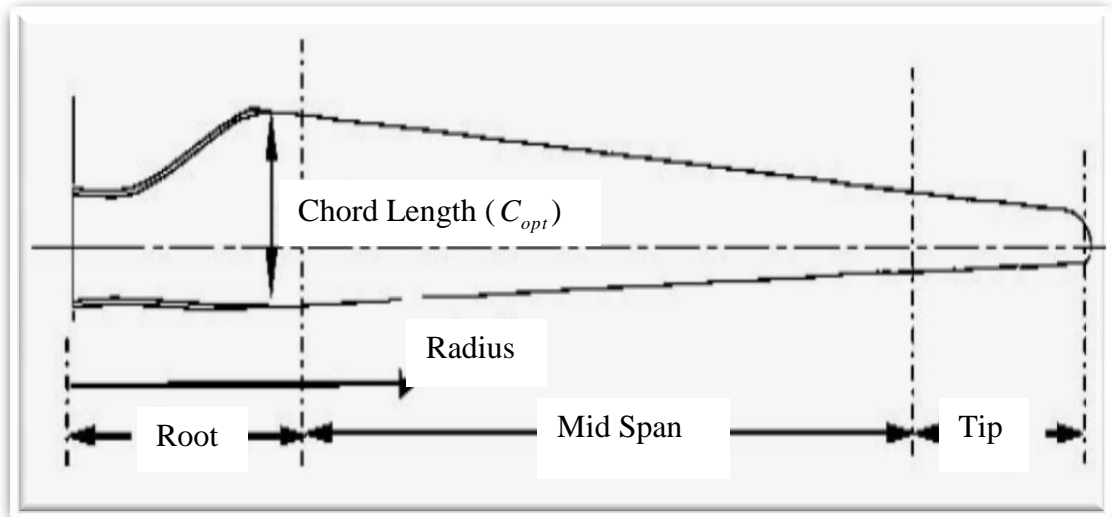


Figure 2.7: A Typical Blade Plan and Region Classification (Hau, 2006).

Practically the chord width is simplified to smooth the progress of manufacture that involves linearization of the increasing chord width (Habali and Saleh, 2000). The author further reported that for superior blade performance, linear deviation of the chord width of a blade can be used between the tip chord and the root chord, though there are efficiency fatalities as a result of simplification to ideal chord length as shown in Figure 2.8. The author in addition cited that for optimum chord dimensioning the magnitude of blades is considered negligible in terms of efficiency.

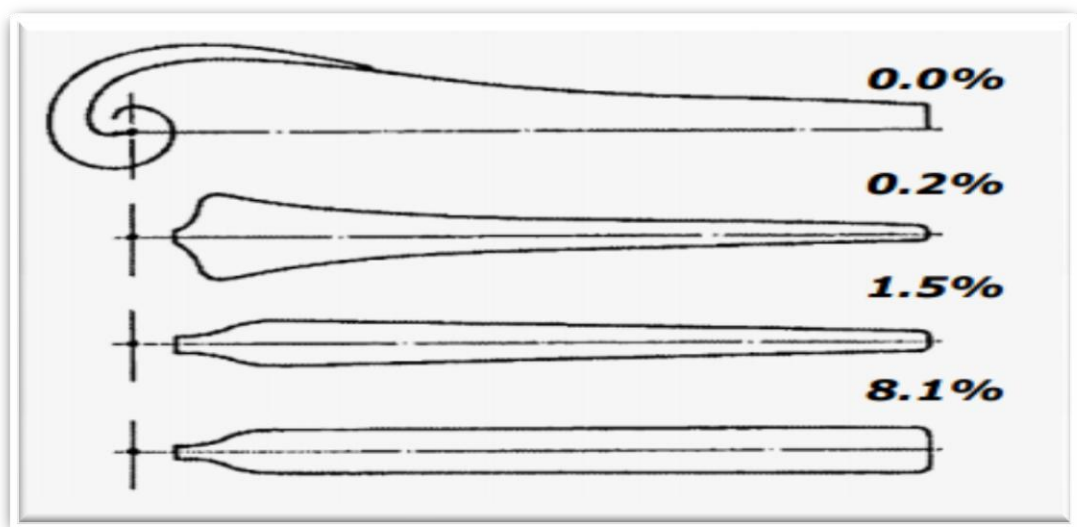


Figure 2.8: Efficiency Losses Due to Ideal Chord Width Simplification (Habali and Saleh, 2000).

In actual fact, when blade losses are considered, about 3 % loss is incurred for two bladed wind turbine design and about 7 % - 13 % loss for one bladed wind turbine when compared to three wind turbine blades design. A four bladed design offers subsidiary efficiency increases which do not give good reason for the manufacturing charge of an extra blade (Habali and Saleh, 2000).

According to Kong et al. (2005), for steady lift over the whole blade length, as blade speed increases toward the tip, the chord of the blade has to decrease as shown in Figure 2.9 (a). The author further reported that an efficient rotor blade *consists* of a number of aerofoil profiles blended at an angle of twist terminating at a rounded flange as shown in Figure 2.9 (b). To smooth the progress of production, some simplifications of blade may be made. These are: reducing the angle of twist, linearization of the chord as well as reducing the number of differing aerofoil profiles as shown in Figure 2.9 (c). The blade as a result tapers from the root to the tip.

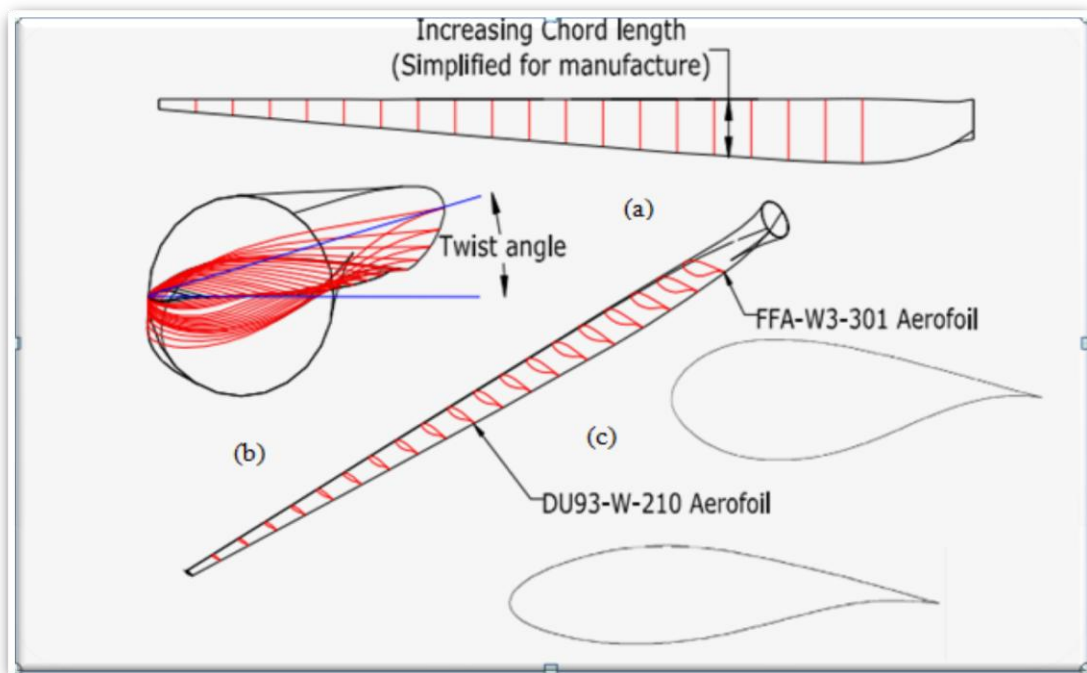


Figure 2.9: A Typical Modern HAWT Blade showing, (a) Linear Chord Length, (b) Twist Angle and (c) Multiple Aerofoil Profiles (Kong et al. 2005).

A mathematical expression for aerodynamically optimum chord width distribution, C_{opt} over the blade span is given by the relation (Hau 2006):

$$C_{opt} = \frac{2\pi \times r}{n} \times \frac{8}{9C_1} \times \frac{V}{\lambda_r V_r} \dots\dots\dots (2.3)$$

where, $V_r = \sqrt{V^2 + u^2}$ is the local effective flow velocity (relative wind speed), u is a tangential wind speed (m/s) and C_1 is local lift coefficient.

According to Ricardo (2001), chord length, C_{Rotor} of a rotor blade whose root chord length and tip chord length are C_{root} and C_{tip} respectively, can be calculated using the relation:

$$C_{Rotor} = \frac{C_{root}(R - r) + C_{tip}(r - 0.14R)}{l} \dots\dots\dots (2.4)$$

where, $l = 0.86R$ is the length of the blade chosen at the location of airfoil, r is the local radius of the rotor as shown in Figure 2.10.

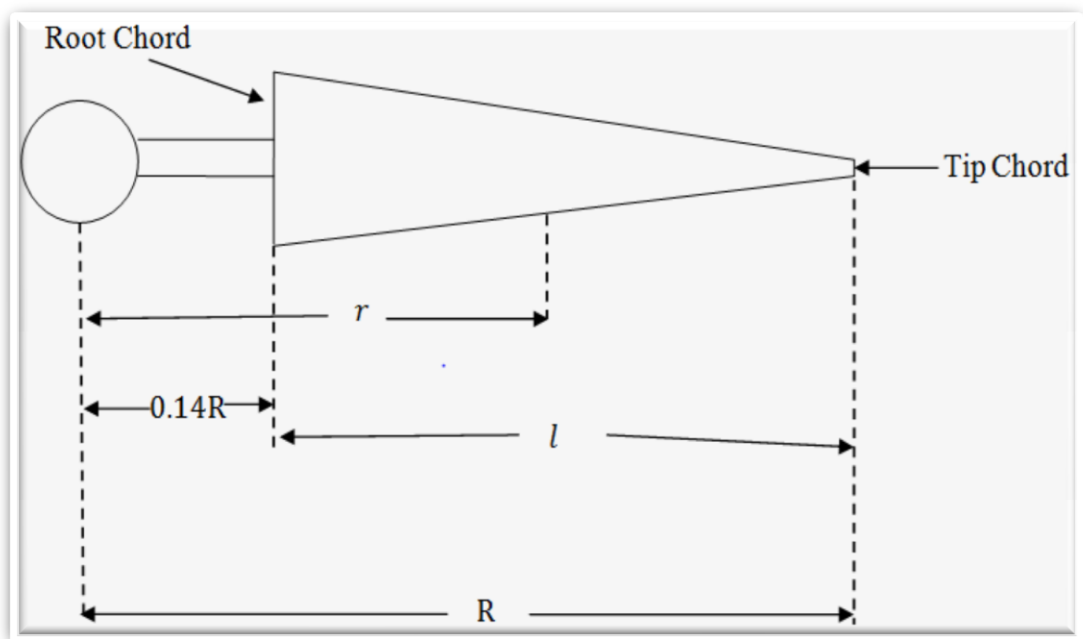


Figure 2.10: Chord Length of a Wind Turbine Blade (Ricardo, 2001).

Equation (2.4) offers constructive outcome for approximated calculation of blade outline. This is only when optimal blade plan shape, optimal TSRs, optimal design and optimal number of blades are used. According to Maalawi and Badr (2003), Betz's momentum theory gives a good quality blade contours estimation with minor drag and tip losses when blades with TSRs of six to nine are used. The use of a single aerofoil for the complete blade length would cause an inefficient blade chord distribution design. Each segment of the blade has a differing relative air pace and so is the structural necessity. Therefore, the root of the blade sections should have large thickness which is important for the intensive loads carried. When impending, the tip blades should blend into thinner sections with condensed load for higher linear velocity and progressively more critical aerodynamic performance. Figure 2.11 shows the optimum chord length distribution which is a hyperbolic function of the blade length.

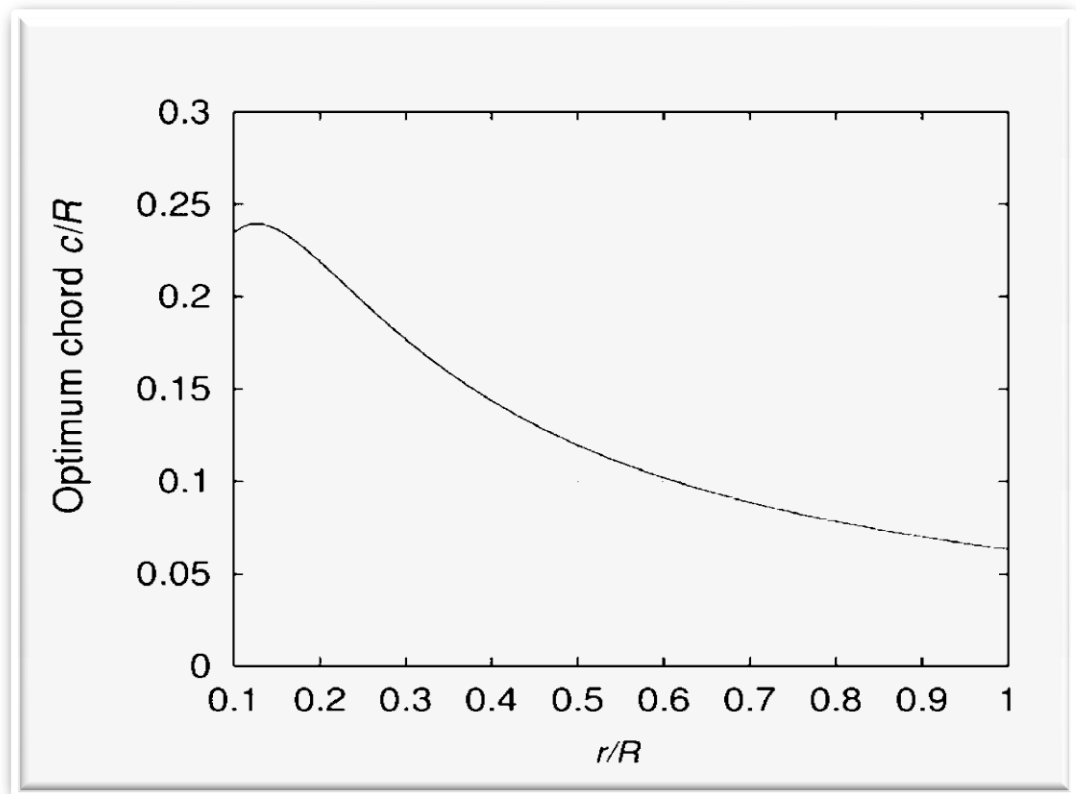


Figure 2.11: Optimum Chord Distribution (Hansen, 2008).

The hyperbolic shapes should be extrapolated to linear relation in order to approximate the required hyperbolic shape as illustrated in Figure 2.12. This linearization intends to develop a blade designed in a tapering manner from the root to the tip in order to allow smooth wind flow from the root chord to the tip chord for improved aerodynamic performance. The optimum efficient shape is always complex because of the aerofoil sections which have a tendency of increasing width, thickness and twist angle towards the hub. This behavior is constrained by physical laws and is unlikely to change (Tony et al. 2001). However, aerofoil lift and drag performance determine exact angles of twist and chord lengths for optimum aerodynamic performance of a wind turbine blade (Tony et al. 2001).

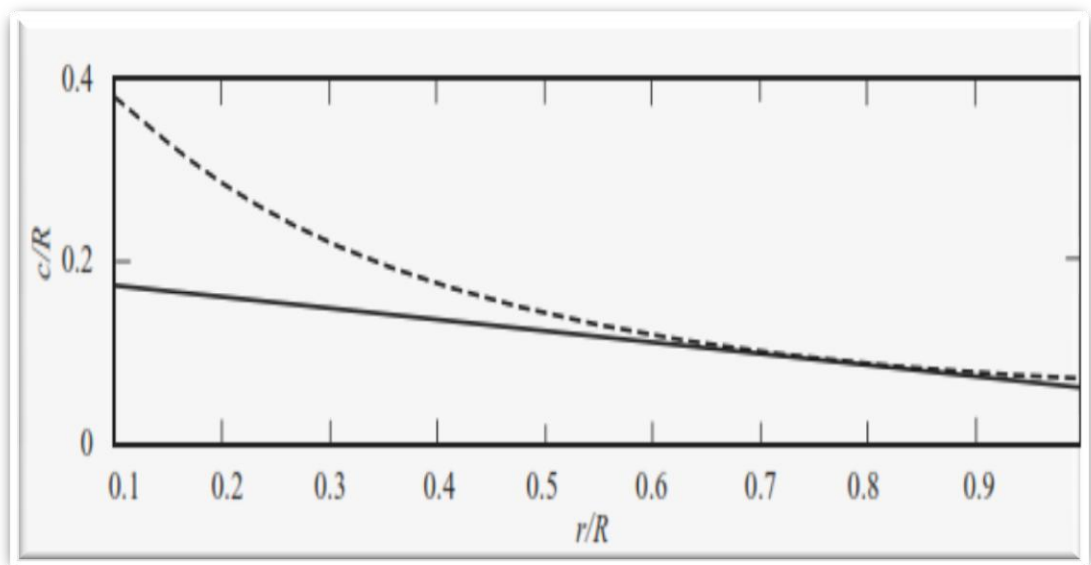


Figure 2.12: Uniform Taper Blade Design for Optimal Operation (Tony et al. 2001).

The linear association of chord c_i distribution with the blade length can be represented by the relation (Tony et al. 2001 and Manwell et al. 2002):

$$c_i = a_1 r_i + b_1 \dots\dots\dots (2.5)$$

where, a_1 , and b_1 are coefficients for the chosen chord distribution. Other symbols are as defined earlier. The trapezoidal plan forms with straight leading and trailing edges proves to be very good guessing for chord distribution (Lindenburg et al. 2001).

Substituting Equation 2.7 into Equation 2.6 gives the relation:

$$\tan\phi = \frac{2}{3\left(1 + \frac{2}{9(\omega^2 r^2)}\right)^2} \omega r \dots\dots\dots (2.8)$$

Geometrically, for a local tip speed ratio, λ_r , $\tan\phi = \frac{1-a}{(1+a')\lambda_r}$, though for the case

when $a' = 0$ (no wake rotation) and $a = \frac{1}{3}$ (the Betz optimum rotor) one obtains (Chen and Shiah, 2016)):

$$\tan\phi = \frac{2}{3\lambda_r} \dots\dots\dots (2.9).$$

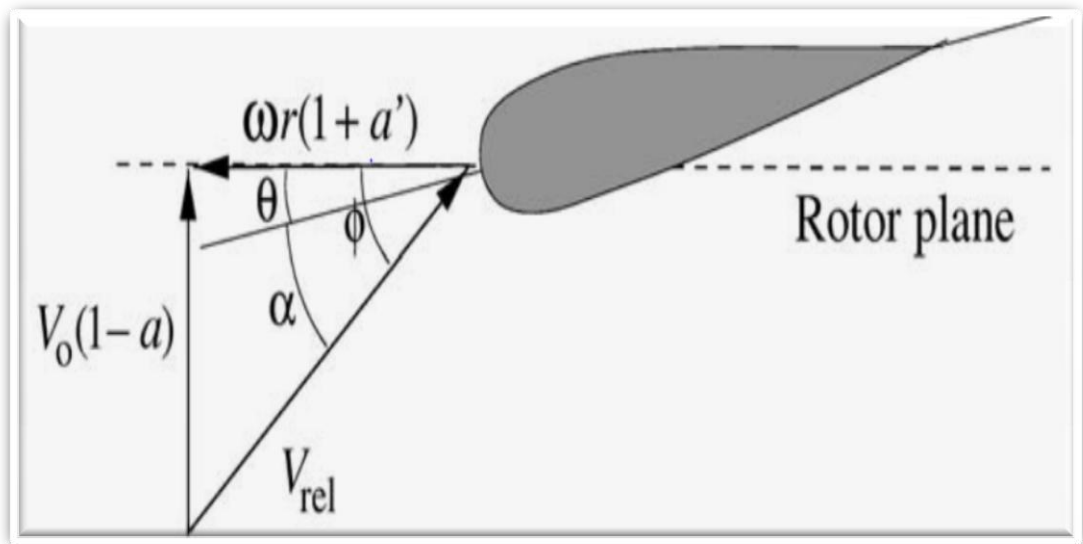


Figure 2.14: Blade Twist Angle and Velocities at the Rotor Plane (Chen and Shiah, 2016).

Making lift coefficient unvarying minimizes drag all over hence, making attack angle uniform at the appropriate value. The variation of the pitch angle then follows as (Chen and Shiah, 2016):

$$\theta = \phi - \alpha \dots\dots\dots (2.10)$$

where, θ is the local pitch angle.

The pitch angle is approximated in such a way that its variation with blade radius is linear as shown in Figure 2.15 with the coefficient a_2 , as shown by the relation (Chen and Shiah, 2016):

$$\theta_{Ti} = a_2(R - r_i) \dots\dots\dots (2.11)$$

where, θ_{Ti} is the local twist angle.

According to Tangler (2000), thickness or rotor blade is a question of rotor blade rigidity and strength requirements. Thicker airfoils have a tendency to be high - lift airfoils and they help the structural integrity of the blade. The root section bears nearly the entire structural load exerted on the wind turbine blade. For constant speed turbines roughness sensitivity increases with airfoil thickness and stall characteristics deteriorate with increasing maximum lift coefficient.

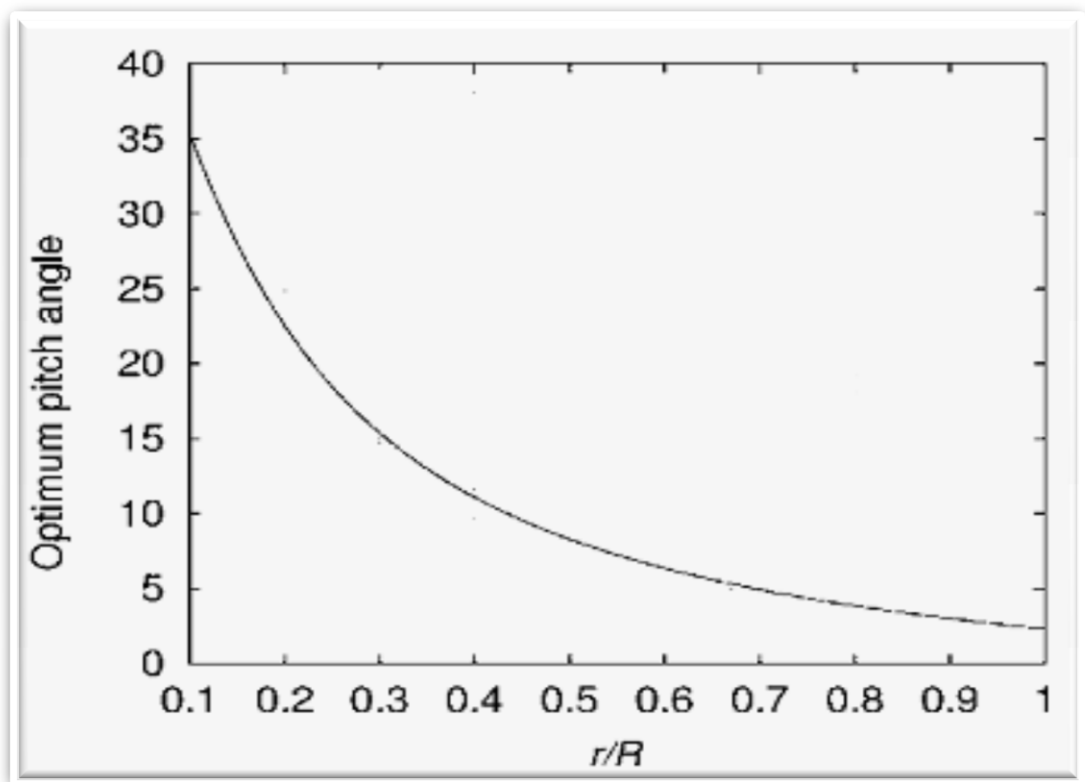


Figure 2.15: Optimum Pitch Angle Distribution (Hau, 2006).

A blade is affected by different forces (loading) during operation. For better performance these forces have to be put under control concern. There are three most noteworthy sources of loading of a wind turbine blade which are gravitational loading, inertial loading and aerodynamic loading (Hansen 2008). Gravitational loading results from the earth's gravitational field that causes sinusoidal gravitational loading on every blade. Figure 2.16 shows that, as the blade are in position 1 that is down - rotating; the blade root at the trailing edge side experiences tensile tension whereas the leading edge side faces compressive stress. Similarly, in position 2 as the blade is up - rotating, the trailing edge side of the blade root is exposed to compressive pressure while the leading edge region is exposed to tensile stress. Therefore, gravity is accountable for a sinusoidal loading of the blades with a frequency analogous to the rotation of the rotor.

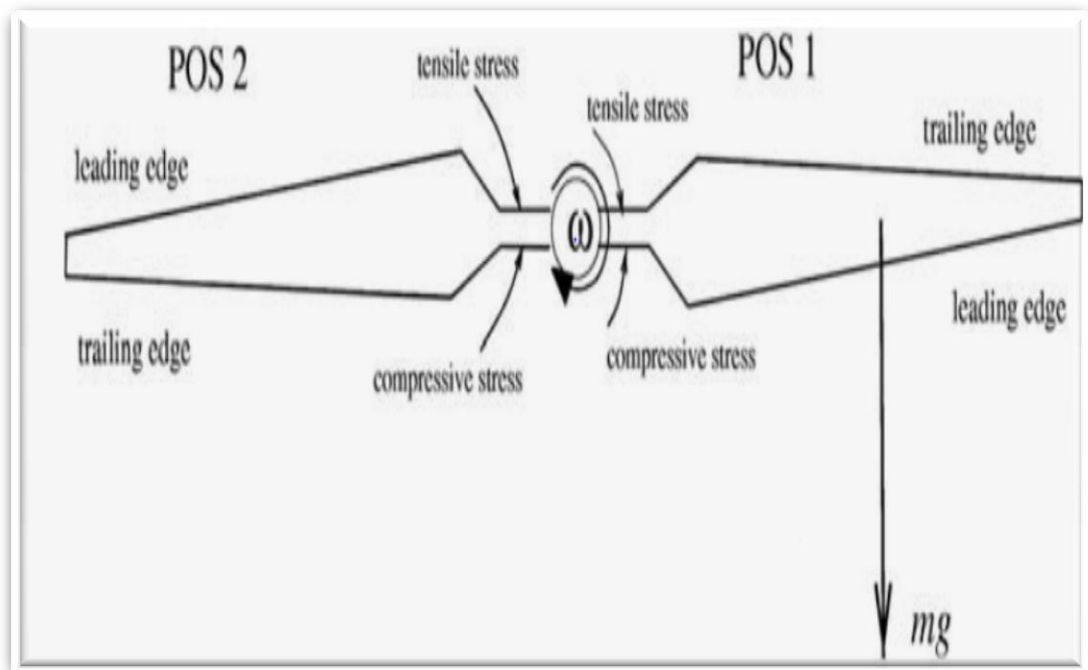


Figure 2.16: Loading Caused by the Earth's Gravitational Field (Hansen, 2008).

Figure 2.17 shows inertial loading which occurs once braking of the rotor takes place by applying braking torque, T at the rotor shaft. This happens when a wind turbine is either accelerated or decelerated. A small part of the blade experiences a small elemental force, dF in the direction of the rotation given as (Hansen 2008):

$$dF = \dot{\omega} r \bar{m} dr \dots \dots \dots (2.12)$$

where, \bar{m} is the mass per length of the blade, r the radius from the rotational axis to the section and dr is the elemental size of the small section. The value of ω can be established from the relation (Hansen 2008):

$$I \frac{d\omega}{dt} = T \dots \dots \dots (2.13)$$

where, I is the moment of inertia of the rotor. In order to decrease bending moment due to quaking, the rotor can be coned backwards with a cone angle of θ_{cone} as shown in Figure 2.18.

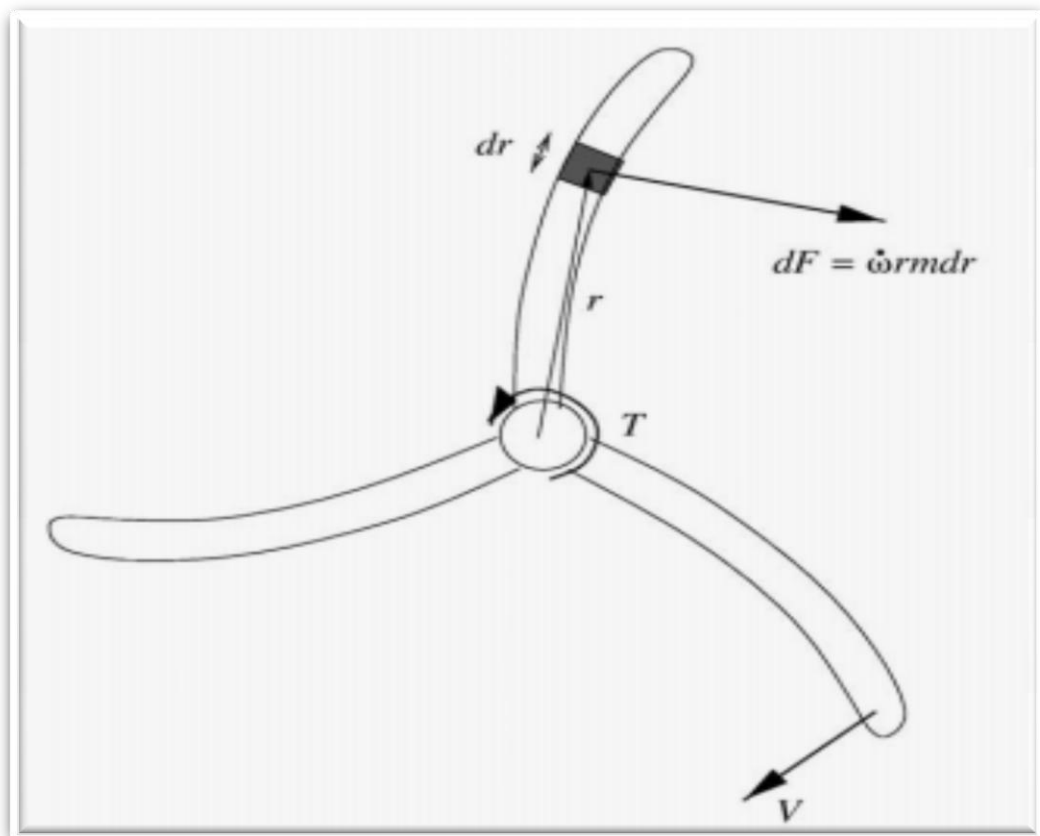


Figure 2.17: Loading Caused by Braking the Rotor (Hansen, 2008).

The centrifugal force acting on the incremental branch of the blade at a radius r from the rotational axis as shown in Figure 2.18 is (Hansen 2008):

$$F = \omega^2 r \bar{m} dr \dots\dots\dots (2.14)$$

where, \bar{m} , is the mass of the incremental part.

Owing to coning, the centrifugal force has a constituent in the span wise direction of the blade, $F_c \cos \theta_{cone}$ and a component normal to the blade, $F_c \sin \theta_{cone}$. The normal factor gives a panic wise bending moment in the opposite direction to the bending moment caused by the push and thus reduces the total flap wise bending moment (Hansen 2008).

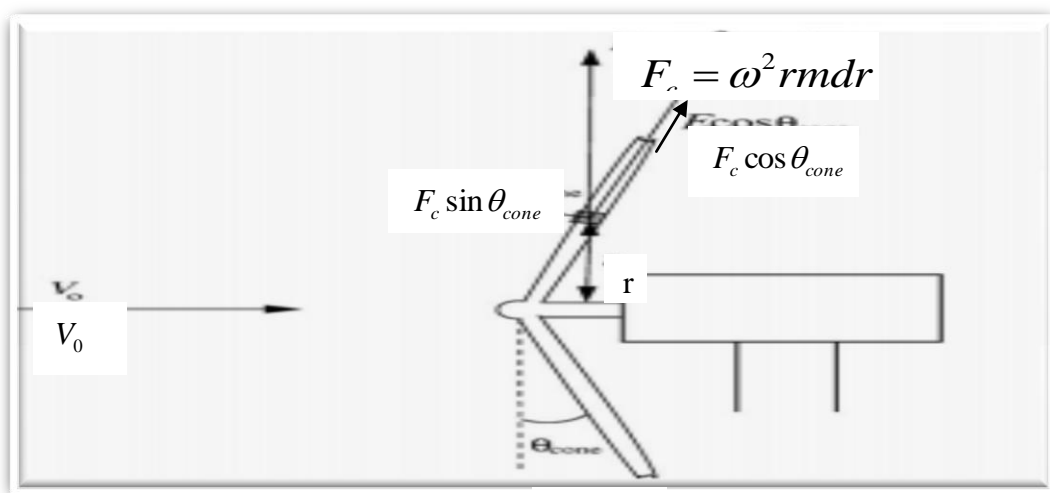


Figure 2.18: Effect of Coning (Hansen, 2008).

The third blade loading is the aerodynamic loading caused by the run past the blades and the tower. The wind stirring at a speed, V_0 seen by the rotor varies in space and time payable to atmospheric instability as indicated in Figure 2.19. This wind field is characterized by shear which implies that the average wind speed increases with the depth above the ground. For neutral stability this shear can be estimated as (Hansen 2008):

$$\frac{V_{10\min}(x)}{V_{10\min}(h)} = \frac{\ln\left(\frac{x}{z_o}\right)}{\ln\left(\frac{h}{z_o}\right)} \dots\dots\dots (2.15)$$

where, $V_{10\min}(x)$ is the time averaged value for a period of 10 minutes at a height x above the ground, $V_{10\min}(h)$ is the time averaged value at a fixed height h , z_o is the roughness length which depends on the surface characteristics and varies from $10^{-4}m$ over water to approximately $1 m$ in cities.

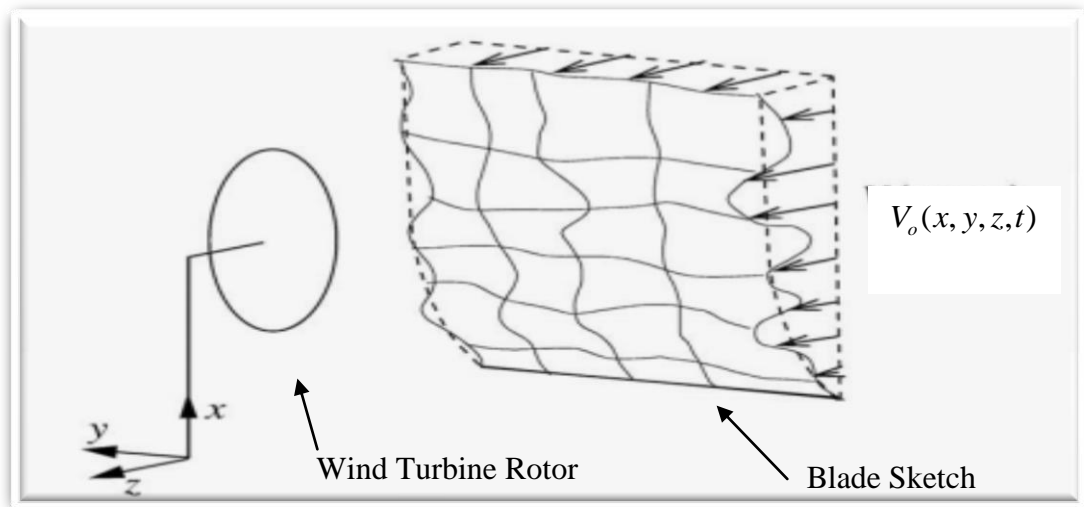


Figure 2.19: Sketch of Turbulent Inflow Seen By Wind Turbine Rotor (Hansen 2008).

2.9 Power Coefficient of a HAWT

Power Coefficient, C_p designates the efficiency of the entire turbine power system. It is generally defined as the ratio of the electrical power produced by the wind turbine divided by the available wind power. The term power coefficient is used by much of the wind power industry to represent the overall efficiency of the turbine. It combines the efficiencies of the blades, mechanical, and electrical components. Knowing the power coefficient at a given wind speed provides a simple approximation of what the actual electrical power produced by the wind turbine will

be. Power coefficient of a wind turbine can be a useful way to compare the performance of a system to a mathematically defined ideal or standard of perfection (Hansen, 2008).

The mechanical power captured by the rotor of a wind turbine is influenced by the geometric shape of the rotor blade (M'endez and Greiner, 2006). The airfoil shape of the blade causes high pressure at the bottom and low pressure at the top. The report by Talam (2011) showed that, the power coefficients increase with decrease in number of blades while solidity is proportional to number of blades and TSR is inversely proportional to the number of blades. The available wind power, p_a is the theoretical power available in a cross section area of a rotor of radius, R . The cross section area is perpendicular to the incoming air of density, ρ moving at a speed, V . The available wind power is given by the relation (Johnson, 2006):

$$p_a = \frac{1}{2} \rho \pi R^2 V^3 \dots\dots\dots (2.16)$$

where the extractable wind power, p_e is the actual power produced by wind turbine and is given by the relation (Johnson, 2006):

$$p_e = \frac{1}{2} \rho \pi R^2 V^3 C_p \dots\dots\dots (2.17).$$

Therefore, power coefficient, C_p is the ratio of the extractable wind power to the available wind power. If all of the power available coming from wind through a turbine were extracted as useful energy then the wind speed behind the rotor would totally drop to zero. If the wind stopped moving at the exit of the rotor then no more fresh wind could get in and the rotor would stop rotating. In order to keep the wind moving through the turbine, there has to be some wind movement, however small, on the other side with some wind speed greater than zero. Betz's law shows that as air flows through a certain area, and as wind speed slows from losing energy to extraction from a turbine, the airflow must distribute to a wider area. For this reason one cannot reduce the wind speed to zero. As a result, there exists a theoretical maximum power coefficient C_p denoted by the Betz limit $C_{p \max} = \frac{16}{27} = 0.593$

(Hansen, 2008). This coefficient signifies that the maximum extracted wind power cannot exceed 0.593.

2.10 Solidity of a Wind Turbine

Solidity σ is the ratio of the actual total area of blades to the swept area of a rotor. Solidity has high influence on the aerodynamic performance of a wind turbine where high solidities cause a turbine to have low power coefficient. Wind turbines perform well close to the Betz's limit for solidities from 0.01 up to 0.05 (Shankar et al. 2016). In this range, turbines have high speed and low torque necessary for required greater tip speed ratios. All wind turbines with solidity above 0.80 have complicated aerodynamic conditions resulting from lower speeds and higher torques (Gipe, 1993). WECS with high solidities have an advantage of self - starting high torques than those with low solidities (Mohamed, 2013). The torque coefficient, C_q at low rotational speeds is directly proportional to the solidity of a wind turbine as shown in Figure 2.20.

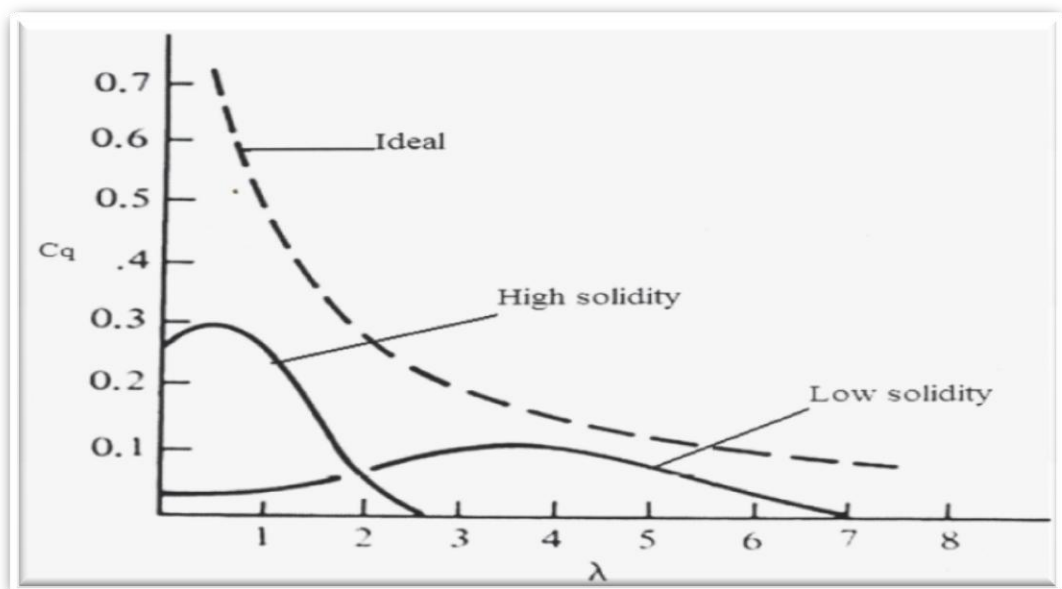


Figure 2.20: Torque Coefficient for TSR Sketched for Large Solidity, Small Solidity and Ideal Criterion (Twidell and Weir, 2006).

The solidities of windmills are higher than that of wind turbines as they are designed for different purposes. Wind turbines generate electricity while windmills grind grains and pump water (Hansen, 2008). Windmills therefore require higher self-starting torques than the wind turbines do. According to Burton et al. (2001), modern high speed wind turbines designed for generating electricity, require low torque. The solidity of a rotor with a varying chord width along the rotor blade is given by the relation (Duquette and Visser, 2003):

$$\sigma = \frac{n \times a}{\pi R^2} \dots\dots\dots (2.18)$$

where, n is the number of blades of a rotor and a is the area of a rotor blade.

According to Hansen (2008) the optimum number of blades for a WECS depends on the purpose of the machine. Three - bladed rotor is the most popular model with a much smoother power output, more efficient and higher power yield, a balanced gyroscopic force and a much better mechanical system compared to the rotors with one blade or two blades. Figure 2.21 shows the influence of number of blades on power coefficient and optimum TSR for different blade rotors.

2.11 Tip Speed Ratio of a Rotor

TSR is used to characterize wind rotors in terms of rotational speed. It depends on the number of rotor blades. The fewer the blades the faster it rotates (Mukund, 1999). Wind turbines for large scale electricity generation have their optimal design Tip Speed Ratios between 4 and 10 (Cetin et al. 2005). A key to designing wind turbine is to assess the optimal tip speed ratio. The power coefficient of a rotor varies with the tip speed ratio and is only a maximum for a unique tip speed ratio (Mok, 2005).

According to the author an optimal TSR implies that the desired power can be generated by a lower torque, which in turn reduces weight of the rotor shaft and gearbox. TSR is defined as the ratio of tip speed of a rotor, ωR to the free stream wind speed V . It is given by the relation (Johnson, 2006):

$$TSR = \frac{\omega R}{V} \dots\dots\dots (2.19)$$

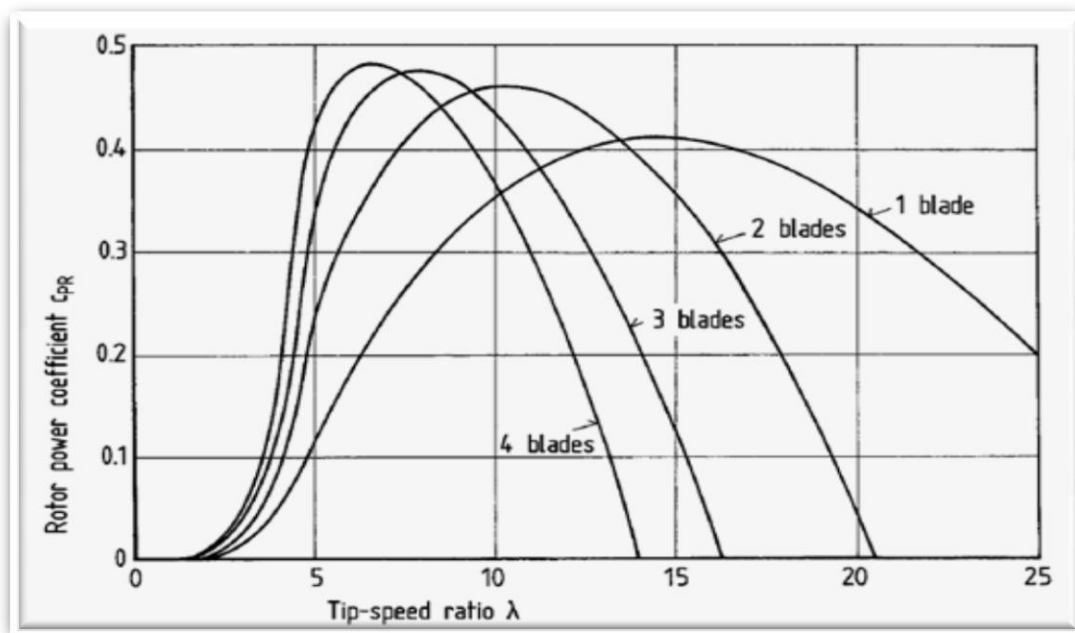


Figure 2.21: Influence of the Number of Blades on Rotor Power Coefficient and Optimum Tip Speed Ratio (Hau, 2006).

where, R is the radius of the wind rotor. The report by Chen and Shiah (2016) on the theoretical modeling of blade design using Blade Element Momentum Theory (BEMT) depicted that the TSR for the HAWT design that was tested was found to be 3.7. The author further showed that TSR, λ_r for each section of the blade can be given by the relation:

$$\lambda_r = \lambda \left(\frac{r}{R} \right) \dots\dots\dots (2.20)$$

where, r is the rotational radius of each blade section and other symbols take their usual meaning. For an n - bladed rotor, it has empirically been observed that the length, S of the disturbed wind stream is approximately equal to 50 % of the rotor radius, R . Thus by setting $\frac{S}{R} = \frac{1}{2}$ then the optimal TSR_{opt} becomes (Cetin et al. 2005 and Ragheb, 2014):

$$TSR_{opt} = \frac{2\pi}{n} \left(\frac{R}{S} \right) = \frac{4\pi}{n} \dots\dots\dots (2.21).$$

Depending on the airfoil used the optimum TSR determined may be 25 - 30 % more than the value obtained using Equation (2.21) because the equation gives non rigorous results (Ragheb, 2014). According to Hau (2006), high TSR entails several problems including drag and tip losses that reduce rotor efficiency, catastrophic failure and even disintegration caused by the run - away turbine due to excessive speed of the rotor, erosion from the impact with dust in the air of the leading edges when a rotor blade rotates at speeds higher than 80 m/s; so, special erosion resistant coatings should be used. The author further depicted that TSR is the determinant of blade shape. For instance, the author recommended that for $TSR < 3$, curved plate blade shapes are suitable while for $TSR > 3$ aerodynamic blade shapes are preferred.

CHAPTER THREE

MATERIALS AND METHODS

3.1 Introduction

This chapter presents the materials and methods used to determine the TSRs, solidities and Re_s , of nine (9) selected locally fabricated HAWTs. Also the chapter presents the methods used for data analysis in relation to the intended objectives.

3.2 Materials

3.2.1 Study Site

Materials used in this study were collected from three centers which are Dar es Salaam, Singida and Makambako. The sites were selected because they have local craftsmen who are known to be engaged in the designing and manufacturing of variety of wind turbines as they are reported in various past researches done on the assessment of wind potential and power efficiency of locally fabricated HAWTs (Talam, 2011 and Msuya, 2015).

3.2.2. Wind Turbine Blades

Three HAWTs with different number of rotor blades as shown in Figures 3.1 to 3.9, were selected from each of the three local wind turbine designing and manufacturing craftsmen namely, Mchau, Matiya and Kyando. TSR, solidity and Re parameters of each blade were determined.

The materials used in designing and manufacturing of the selected local wind turbines are diverse. The wind turbine blades as shown in Figure 3.1 are made of simple aluminium sheets while those in Figures 3.2 to 3.6 are made of plastic materials. Furthermore, the wind turbines shown in Figures 3.7 to 3.9 are made of scrapers of steel materials. Most of the local wind turbines used Plastic materials because aluminium is more expensive despite being a non ferrous metal with lower density and high ability to resist corrosion (Gipe 1995).



Figure 3.1: 6 - Bladed HAWT. Source: Mchau, 2018.



Figure 3.2: 8 - Bladed HAWT. Source: Mchau, 2018.



Figure 3.3: 20 - Bladed HAWT. Source: Mchau, 2018.



Figure 3.4: 3 - Bladed HAWT. Source: Matiya, 2018.



Figure 3.5: 4 - Bladed HAWT. Source: Matia, 2018.



Figure 3.6: 5 - Bladed HAWT. Source: Matiya, 2018.



Figure 3.7: 16 - Bladed HAWT. Source: Kyando, 2018.



Figure 3.8: 18 - Bladed HAWT. Source: Kyando, 2018.



Figure 3.9: 14 - Bladed HAWT. Source: Kyando, 2018.

3.3 Methods for Determination of TSR, Solidity and Re Parameters

The optimal TSR of each of the selected local wind turbine blades was determined using Equation (2.21). The influence of TSR to the aerodynamic performance of the local turbines was assessed by comparing measured TSRs with the standard values shown in Table 3.1.

Table 3.1: Recommended Blade Design Parameters for Large Scale Electricity Generation

S/NO	Parameter	Symbol	Recommended Value
1	TSR	λ	4 to 10 (Cetin et al. 2005)
2	Solidity	σ	0.01 to 0.05 (Shankar.et al. 2016)
3	Reynolds Number	Re	At least 1×10^6 (Hansen, 2008)

This comparison aimed at evaluating the efficiency of the selected local HAWTs for improvement of their rotor blades performances. High TSR is the most required design parameter for obtaining good efficiency of a wind turbine although its blade tip speed must not exceed 80 m/s above which the rotor blade exhibits noise and erosion due to collision with atmospheric aerosols (Ragheb, 2014).

Determination of solidity of blades for each of the selected HAWTs was done by substituting area of a rotor blade a , number of rotor blades, n and rotor area, A , in Equation (2.18). The area of a rotor blade was taken as the product of blade length, l and chord width, c of the rotor blade assuming the rotor blade to be rectangular shaped. To determine the effect of solidity on the aerodynamic performance of the selected local HAWTs, the measured solidity values were compared with the recommended standard values.

Computation of Re was attained by measuring and entering the chord width, c of each selected local HAWT rotor blade into the XFOIL program to calculate Re (<http://www.airfoiltools.com>). All selected WECS were assumed to operate at a wind speed of 10 m/s at a height of 10 m Above the Ground level (AGL) for reasonable comparison of measured Re values. The corresponding kinematic viscosity of air was taken $1.5111 \times 10^{-5} m^2/s$ (<http://www.airfoiltools.com>). To assess the influence of Re on the selected local HAWTs, the measured Re_s were compared with the recommended standard Re .

XFOIL (<http://www.airfoiltools.com>) is an interactive program for the design and analysis of subsonic isolated airfoils that is used in plotting geometry by interactive modification of geometric parameters. It uses many NACA series but, in this study NACA 63-415 was used to calculate Re because it exhibits better lift to drag ratio close to 120 (Hansen, 2008). Microsoft Excel was used to plot graphs of measured TSRs, solidities and Re of the selected local HAWTs in comparison with the recommended standard TSR, solidity and Re values.

CHAPTER FOUR

RESULTS AND DISCUSSIONS

4.1 Introduction

This chapter presents results and discussion of examined aerodynamic performances of the nine (9) selected HAWTs from three centers. In this chapter, the influence of TSR, solidity and Re on the aerodynamic performance of the selected locally fabricated HAWTs was assessed.

4.2 Measured Parameters of Local HAWTs

Table 4.1 displays the measured TSRs, solidities and Re_s of the selected local HAWTs. The table shows also the number of rotor blades, n , area of a rotor blade, a , radius of the blade, R , area described by the rotor, A and chord width of the blade, c used in determination of TSRs, solidities and Re_s values.

Table 4.1: Measured TSRs, Solidities and Re_s of Local HAWTs

Figure	N	R (m)	l (m)	A (m ²)	c (m)	a (m ²)	TSR	Solidity	Re
3.1	6	1.22	1.05	4.68	0.13	0.14	2.09	0.18	86,030
3.2	8	1.38	1.12	5.98	0.19	0.21	1.57	0.28	125,736
3.3	20	1.36	1.17	5.81	0.22	0.26	0.63	1.90	145,589
3.4	3	1.20	1.03	4.53	0.150	0.15	4.19	0.10	99,265
3.5	4	1.25	1.06	4.90	0.152	0.16	3.14	0.13	100,589
3.6	5	1.23	1.06	4.75	0.155	0.16	2.51	0.17	102,574
3.7	16	0.90	0.77	2.54	0.22	0.17	0.79	1.07	145,589
3.8	18	0.92	0.79	2.66	0.23	0.18	0.70	1.22	152,207
3.9	14	0.90	0.77	2.54	0.21	0.16	0.90	0.88	138,972

4.2.1 Measured TSRs

From Table 4.1, TSRs were found to be 0.63, 0.70, 0.79, 0.90, 2.09, 1.57, 2.51, 3.14 and 4.19 with regards to Figures 3.1 to 3.9. These results are also represented by a histogram shown in **Appendix 4A** for comparison with the recommended TSR for

which wind turbines are designed to generate large scale electricity. The wind turbine shown in Figure 3.4 was found to have a TSR of 4.19 which is in the recommended range of 4 to 10 as shown in Table 3.1. The reason for this agreed value is due to the fewer number of blades compared to other wind turbines. Few numbers of blades signify low solidity leading to low power efficiency (Cetin et al 2001). The rest low TSR values imply that the rotor blades of the selected locally fabricated WECS have low tip speeds which as a result influence low aerodynamic performances (Cetin et al 2001).

4.2.2 Measured Solidities

From Table 4.1, the solidity values measured were 0.10, 0.13, 0.17, 0.18, 0.28, 0.88, 0.90, 1.07 and 1.22. The results are also represented in a histogram shown in the **Appendix 4B** for comparison of the measured solidities with the recommended solidities for which wind turbines are designed to generate large scale electricity. The table shows that as the blade number increases, the rotor blade load increases and solidity of wind turbine increases proportionally.

The measured solidities are all above the recommended range of 0.01 to 0.05 as illustrated in Table 3.1. According to (Cetin et al 2001) and Talam (2011), high solidities reduce TSR leading to low aerodynamic performance of the WECS. The table shows that the highest solidity values measured were 1.07, 1.22, 1.43 and 0.88 and they place their respective WECS into a group of windmills for grinding grains or pumping water purpose (Shankar et al, 2005). The reason for high values is due to large area covered by the blades of the WECS which results into low speeds due to high torques contrary to the necessary required greater TSRs. High torques cause high drag coefficients where the WECS experience heavy load for rotation (Gippe, 1995).

4.2.3 Measured Re

From Table 4.1, the measured Re , with respect to Figures 3.1 to 3.9 were 86,030, 99,265, 100,589, 102,574, 125,736, 138,972, 145,589, 145,589 and 152,207. These results are also represented in a histogram shown in **Appendix 4C** for comparison of

this study Re results with the recommended Re for which WECS are able to stall (change from lamina to turbulent flow). According to Tony et al. (2001), for high Re , viscous forces are low and vice versa. The measured Re values are below the recommended Re which is at least 1×10^6 meaning that the WECS experience high viscous forces that influence turbulent flow regime with low level of lift coefficient leading to low aerodynamic performance of the selected locally fabricated wind turbines. These lower values might be caused by poor design chord widths distribution and bad shapes of the rotor blades of local WECS which are not airfoil shaped. There are no other reports done on Re in Tanzania to be used for comparison with the results of this study.

Low TSR, high solidity and low Re , reveal that the WECS have low efficiency and as a result the selected locally fabricated wind turbines will show low efficiency when measured at the same RPM in comparison with standard ones because of their low TSR values as stipulated by other studies (Cetin et al, 2001). The low efficiency is the influence of poor geometry of the locally fabricated wind turbines and manifests low aerodynamic performance of the locally fabricated wind turbines. For example Msuya (2015) in his simulation experiment of two generators, one local generator and one standard generator with 8 and 6 pole pairs respectively, he reported that the Tanzanian locally fabricated generator had low efficiency since it recorded 55 % efficiency while the standard one recorded 96 % efficiency while both were set at 350 RPM. The author further reported that the generator with six pole pair was better than the 8 pole pair by 31 %.

4.2.4 Comparison of this Study Results with Other Studies in Tanzania

Table 4.2 provides the comparison of the measured TSR, Solidity and Reynolds numbers of this study with other studies in Tanzania on the locally fabricated wind turbines.

The reports by Talam, (2011) and (Msuya, 2015) in Tanzania also revealed that the locally fabricated wind turbines have low aerodynamic performance as this study found, though Msuya (2015) dealt with efficiency rather than measuring TSR and

Solidity. The results of this study are in agreement with results of the authors Talam and Msuya, that both results are higher than the recommended ones. For instance, Talam, (2011) assessed the power output characteristics of two HAWT, one with a rotor of 5 blades and the other with 16 blades and found that the machines exhibited low power coefficients of 0.14 and 0.21 at low TSRs of 0.61 and 1.7 while this study measured respectively 2.51 and 0.79. He also obtained high solidities of 0.5 and 0.29 at the same low power coefficients of 0.14 and 0.21 of the same turbines under test. The author reported that the solidities were so high compared to that of modern HAWTs which are recommended to be less than 0.07 with power coefficient in the optimal range of 0.4 to 0.5 (Cetin et al, 2005). Consequently, the author recommended improving the aerodynamic efficiencies of these locally fabricated machines by enhancing the interaction between scientists, engineers and indigenous technicians.

Table 4.2: Comparison of Measured TSR, Solidity and Re with Other Studies in Tanzania

Present Study				Other Studies			
<i>n</i>	TSR	Solidity	<i>Re</i>	TSR	Solidity	<i>Re</i>	Other Authors
3	4.19	0.10	99,265				None
4	3.14	0.13	100,589				None
5	2.51	0.17	102,574	0.61	0.5		Talam (2011)
6	2.09	0.18	86,030				None
8	1.57	0.28	125,736				None
16	0.79	1.07	145,589	1.7	0.29		Talam (2011)
18	0.70	1.22	152,207				None
14	0.90	0.88	138,972				None
20	0.63	1.90	145,589				None

Both TSR and solidity values in his report differ with that of this study. The reason might be because he used experimental approach while this study used theoretical approach. He rotated the turbines manually to be able to count the number of RPM

implying that he performed the experiment under very low speeds. If he had used high speeds and high frequency (non manual) his results would approach the values from this study which used optimization standard theories. Just as this study has found, the author also found that the lower TSR and higher solidity values of the selected wind turbines were not suitable for large scale electricity generation because they were out of the optimal design range implying that they influence low aerodynamic performance.

In summary the 3-bladed wind turbine shown in Figure 3.4 had TSR which is in the range of proposed design values of 4 to 10, although its solidity value is a bit above the recommended value range of 0.01 to 0.05. If its chord width distribution and the radius were optimized to bring down the solidity then it could yield higher aerodynamic performance and be used for generation of large scale electricity. All measured solidities were above the standard value, while all Re values were below the recommended standard value which is at least 1×10^6 . Therefore, the low TSR values, low Re values and high solidity values influence low aerodynamic performance of the selected WECS.

CHAPTER FIVE

CONCLUSIONS AND RECOMMENDATIONS

5.1 Introduction

This chapter presents conclusions and recommendations following the nature of the results of computed TSR, solidity and Re values of nine selected locally fabricated HAWTs.

5.2 Conclusions

Among the selected HAWTs, only the 3 - bladed wind turbine exhibited a TSR value of 4.19 which is within the recommended range of 4 to 10 while the rest values were below. This TSR therefore, has high influence on good aerodynamic performance of the 3-bladed wind turbine compared to others. The rest selected locally fabricated wind turbines measured TSRs below the recommended range. They therefore cause the turbines to experience low rotational speeds thereby influencing low aerodynamic performance of the machines. The measured solidities had higher values which cause the wind turbines to be too slow in rotation. These high solidities reduce efficiency of the turbines resulting into low aerodynamic performance too. The Reynolds numbers Re , measured are also low compared to the standard ones hence causing airflow past the blade inefficient for the turbine to harvest more power. Generally, the measured low TSR values, measured high solidity values and measured low Re values all together influence low aerodynamic performance of the selected HAWTs. Therefore, the selected WECS can only be used for small scale electricity generation.

5.3 Recommendations

It is recommended that the craftsmen need to interact with scientists and engineers to exchange knowledge of optimal number and shape of rotor blades which have direct effect on the design TSR, solidity and Re parameters. It is proposed that further researches be conducted on the following areas; Firstly, determination of optimal TSR and solidity parameters of 3 - bladed local HAWT by measuring its power coefficient for specific wind velocity. Secondly, optimization of the aerodynamic blade designs of locally fabricated HAWTs based on the shape, size and number of blade.

REFERENCES

- Burton T, Sharpe D, Jeckins N and Bossany E 2001 *Wind Energy Handbook*: John Willey and Sons Ltd. Chichester, UK.
- Cagle D, Mays A, Vick BD and Holman A 2007 Evaluation of Airfoils for Small Wind Turbines In Proceedings of the AWEA Wind power Conference, June 3-6, 2007, Los Angeles California 2007 CD-ROM.
- Cetin NS, Yurdusev MA, Ata R and Ozdemir A 2005 Assessment of Optimal Tip Speed Ratio of Wind Turbine. *Journal of Mathematical and Computational Application*, **1**: 147–154.
- Chattot JJ 2003 Optimization of Wind Turbines Using Helicoidal Vortex Model, *J. Sol. Energy Eng. Trans. ASME*, **125**, 418-424.
- Chen Y and Shiah YC 2016 Experiments on the Performance of Small Horizontal Axis Wind Turbine with Passive Pitch Control by Disk Pulley. MDPI AG, Switzerland.
- Duquette MM and Visser KD 2003 Numerical Implications of Solidity and Blade Number on Rotor Performance of Horizontal-Axis Wind Turbines, *J Sol Energy Eng.-Trans. ASME*, **125**, 425-432.
- Eke GB and Onyewudiala JI 2010 Optimization of Wind Turbine Blades Using Genetic Algorithm. *Journal of research in engineering*, **10**: 22 – 24.
- Gipe P 1993 *Wind Power for Home and Business and Renewable energy for the 1990s and beyond*. Post Mills, VT Chelsea Green publishers, London.
- Habali SM and Saleh IA 1995 Design and Testing of Small Mixed Airfoil Wind Turbine Blades. *Renewable Energy*, **6**(2):161-169.
- Habali SM and Saleh IA 2000 Local Design, Testing And Manufacturing Of Small Mixed Airfoil Wind Turbine Blades of Glass Fiber Reinforced Plastics

Part I: Design Of The Blade And Root. *Energy Convers, Manag*, **41**: 249 - 280.

Hansen AC and Butterfield CP 1993 Aerodynamics of Horizontal-Axis Wind Turbines Annual Review. *Journal of Fluid Mechanics*, **25**:115-149.

Hansen MOL 2008 General Introduction to Wind Turbines (2nded): Earth scan, UK and USA.

Hau E 2006 Wind Turbines: Fundamentals, Technologies, Applications, and Economics (2nded): Springer, Berlin, Germany.

Jansen WAM and Smulders PT 1977 Rotor Design For Horizontal Axis Windmills. SWD publications Vol. 7701. Amersfoort, Stuurgroep Windenergie Ontwikkelingslanden.

Johnson GL 2006 Wind Energy Systems. University reprints, Amazon.

Kihedu J 2007 Assessment of Wind Energy Potential and Application in Tanzania. Msc Physics Dissertation, University of Dar es Salaam.

Kong C, Bang J and Sugiyama Y 2005 Structural Investigation of Composite Wind Turbine Blade Considering Various Load Cases and Fatigue Life. *Energy*, **30**: 2101-2114.

Kumwenda M 2011 Assessment of Wind Potential for Electric generation at Kititimo in Singida Region. Msc. Physics Dissertation, University of Dar es Salaam.

Lindenburg C, Bot E and Hendriks HB 2001 Aerodynamic Parameter Sensitivity Study. ECN-C--00-077, ECN, Petten.

Maalawi KY and Badr MA 2003 A Practical Approach for Selecting Optimum Wind Rotors. *Renewable Energy*, **28**, 803 - 822.

- Manwell JF, McGowan JG and Rogers AL 2002 *Wind Energy Explained Theory Design and Application*, John Wiley and Sons Ltd.
- M'endez J and Greiner D 2006 *Wind Blade Chord and Twist Angle Optimization Using Genetic Algorithms: Fifth International Conference on Engineering Computational Technology*, Las Palmas de Gran Canaria, Spain.
- Mohamed MH 2013 *Impacts of solidity and hybrid system in small wind turbines performance*, **57:09**.
- Mok K 2005 Identification of the Power Coefficient of Wind Turbines: Proceedings of the 45th IEEE Conference on Decision and Control, **2**: 2078 – 2082.
- Mukund RP 1999 *Wind and Solar Power Systems*. CRC Press, Amazon.
- Msuya RA 2015 *Determination of Power Efficiency of Locally Fabricated Wind Turbine Generators in Tanzania*. PhD in Physics Thesis, University of Dar es Salaam.
- Mwanyika HH 2005 *The potential of wind based energy for electricity generation at Makambako –Iringa, Tanzania* MSc. Dissertation, University of Dar es Salaam.
- Nzali A and Mush S 2006 *Wind Energy Utilization in Tanzania*. PREA Workshop Proceedings.
- Ragheb M 2014 *Optimal Rotor Tip Speed Ratio*. <http://mragheb.com/NPRE%200475%20Wind%20Power%20Systems/Optimal%20Rotor%20Tip%20Speed%20Ratio.pdf>.
- Ricardo B 2001 *A Simple Calculation of Chord Length of A Wind Turbine*, <http://www.Ricardo Bastonion>. *Googlepages.com* retrieved on Monday, 4th May, 2010.
- Shankar RN, Stanly D, Manikandan AA and Raja SJI 2016 *Design and Fabrication of Horizontal Axis Wind Turbine*. International Conference on

Mechanical, Materials and Manufacturing Engineering. Chennai, Vels University.

Shimizu YW, Takada M and Sakata J 1998 Development of High Performance Crossflow Wind Turbine. *Transactions of JSME series B*, Volume 64, No 625.

Spera DA 1998 Wind Turbine Technology. Asme Press, New York.

Talam KE 2011 Assessment of Performance Characteristics of Some Stand Alone Small Scale Wind Turbines Fabricated in Tanzania. MSc. (Physics) Dissertation, University of Dar es Salaam.

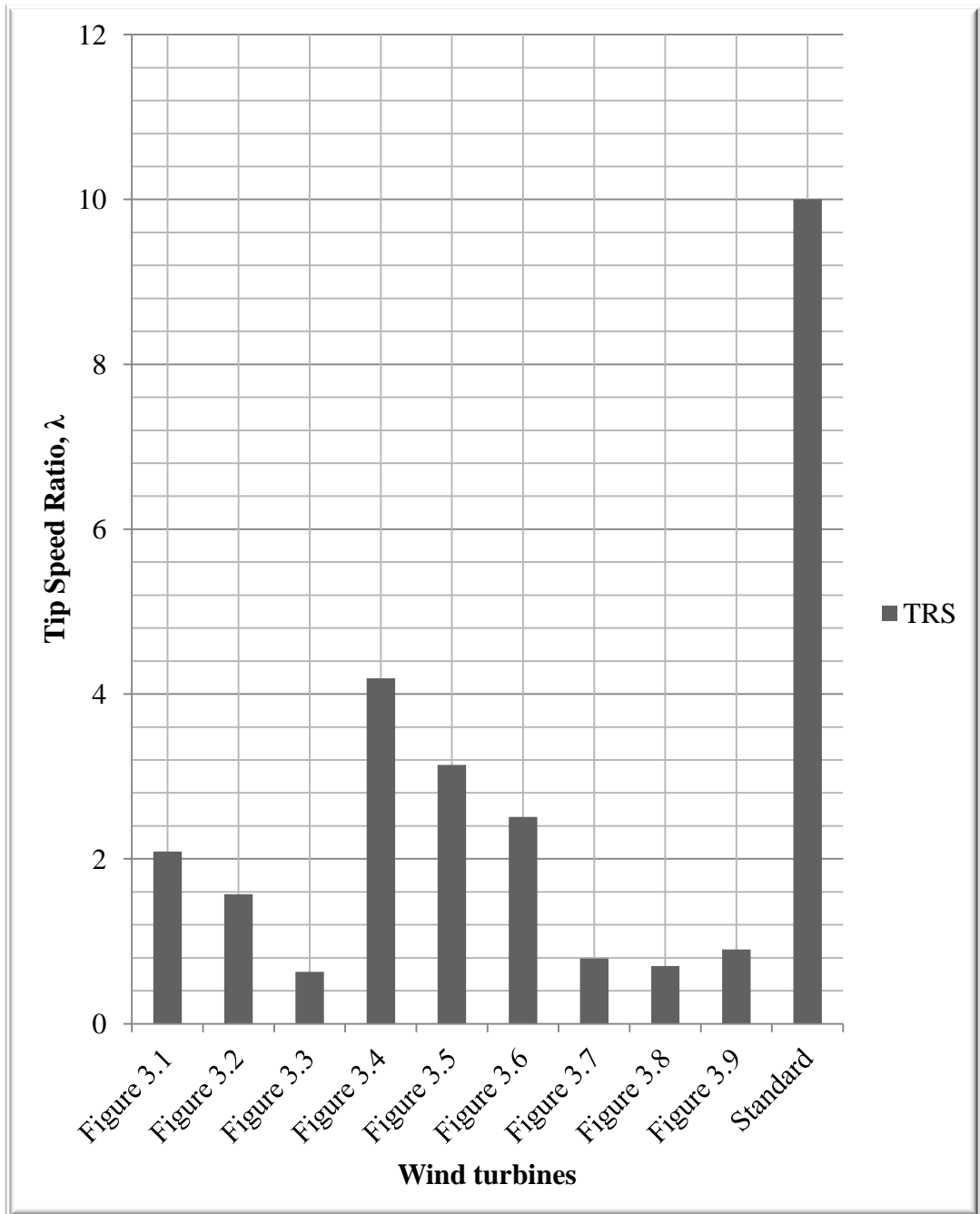
Tangler JL 2000 The Evolution of Rotor and Blade Design, American Wind Energy Association, Wind Power Conference Proceeding, California.

Tony B, David S, Nick J and Ervin B 2001 Wind Energy Hand book. John Wiley and Sons, Ltd, Chichester.

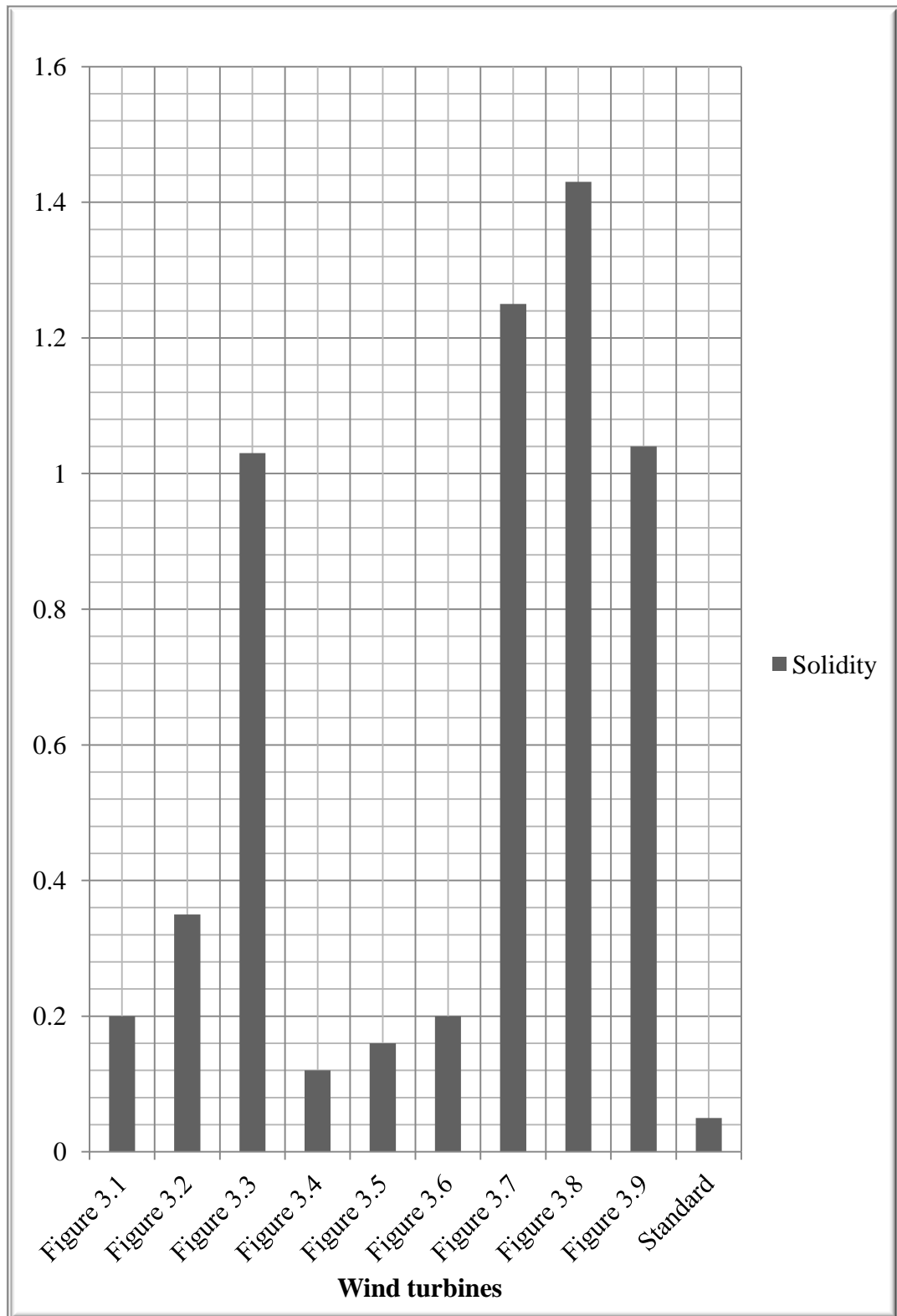
Twidell J and Weir T 2006 *Renewable Energy Resources 2nd* (Ed), Taylor and Francis.

Wagner H 2012 New Strategies for Energy Generation, Conversion and Storage Research to International School on Energy. Villa Monastero, Varenna (Lake Como).

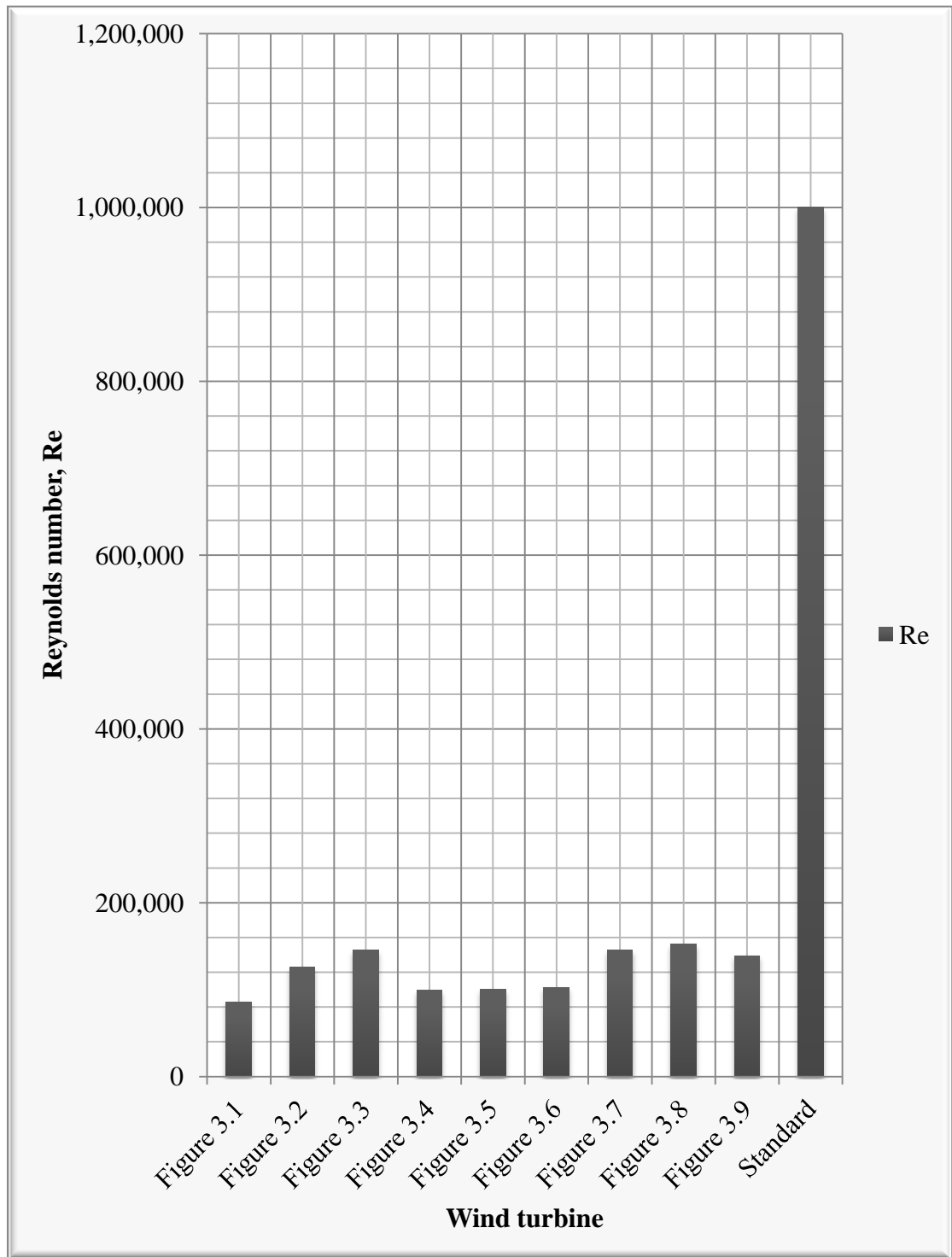
APPENDICES



Appendix 4A: A Histogram of TSRs for Standard and the Selected Local HAWTs.



Appendix 4B: A Histogram of Solidities for Standard and the Selected Local HAWTs.



Appendix 4C: A Histogram of Re_s for Standard and the Selected Local HAWTs